4

Conventional flux balance analysis and its applications

Abstract: The conventional flux balance analysis method is briefly explained. Its application to the metabolic flux analysis of the *Chlorella* cell, under autotrophic, heterotrophic, and mixotrophic conditions, focuses on energy generation. Other applications to such single-gene knockout *Escherichia coli* strains, such as *pflA*, *pta*, *ppc*, *adhE*, and *pykF* mutants cultivated under anaerobic conditions, are also explained, as is metabolic regulation analysis based on metabolic fluxes, enzyme activities, and intracellular metabolite concentrations.

Key words: flux balance analysis; *Chlorella* cell; *pflA* mutant; *pta* mutant; *adhE* mutant; *ppc* mutant; *pykF* mutant; anaerobic conditions; photosynthetic bacteria.

4.1 Introduction

It is important to clarify metabolic fluxes in practice, where a set of metabolic fluxes describe the cell physiology. The information on metabolic flux distribution is useful in metabolic engineering (Bailey, 1991; Stephanopoulos and Vallino, 1991; Stephanopoulos, 1999). In principle, metabolic flux analysis is based on mass conservation of key metabolites. Intracellular fluxes can be calculated from the measured specific rates by applying mass balances to these intracellular metabolites together with stoichiometric equations. The number of measurable extracellular fluxes is limited in practice, and the stoichiometric constraints often lead to an underdetermined algebraic system. Therefore, cofactor balances sometimes need to be introduced into the stoichiometric model, or the appropriate objective functions have to be introduced for optimization to determine the fluxes.

Published by Woodhead Publishing Limited, 2013

The central metabolic pathway has both anabolic and catabolic functions, as it provides cofactors and building blocks for macromolecular synthesis (anabolism), as well as energy (ATP) generation (catabolism). Optimization may be made in terms of catabolism and anabolism, or both, under the constraints of the stoichiometric equations. Flux balance analysis (FBA) has been extensively used to predict steady-state metabolic fluxes in order to maximize cell growth rates (Schilling and Palsson, 1998; Edwards and Palsson, 2000; Price and Papin, 2003). This method has been significantly extended to genome-scale models which include thousands of metabolic reactions (Palsson, 2009). *E. coli* utilizes carbon almost optimally, and this is a special feature of this organism (Edwards et al., 2001; Ibarra et al., 2002; Yuan et al., 2006).

However, the accuracy of the flux calculation depends on the validity of the cofactor assumptions and an appropriate choice of the objective function(s) employed (Schuetz et al., 2007). The presence of unknown reactions that generate or consume the cofactors may invalidate the assumption that their concentrations remain in balance, and the selected objective functions may not be appropriate, or their validity may be limited to certain states of the cell. Note that this approach cannot essentially compute such fluxes as: i) recycled fluxes; ii) bidirectional fluxes; and iii) parallel fluxes, due to the singularity of the stoichiometric matrix. These fluxes can be computed based on ^{13}C-matabolic flux analysis, which is explained in Chapter 5. Note, however, that the conventional FBA may be reasonably applied for cases without recycles, such as anaerobic or microaerobic cultivation or by lumping several pathways together. Here we consider metabolic flux analysis based on mass balances with stoichiometric equations and show its several applications.

4.2 Basis for metabolic flux analysis

As shown by Figure 1.1, when using glucose as a carbon source, the overall main metabolic reactions under aerobic condition may be expressed as:

$$\text{Substrate} + \text{nitrogen source} + O_2 \rightarrow \text{biomass} + \text{metabolites} + CO_2 + H_2O \quad (4.1)$$

Let r_i be the specific consumption or production rate of the *i*th substance, and let E be the stoichiometric matrix. Then the following mass balance holds at steady state, where the specific rate is defined as the consumption or production rate of the substance of interest per cell per hour:

$$E \cdot \mathbf{r} = 0 \quad (4.2)$$

Published by Woodhead Publishing Limited, 2013

where $\mathbf{r}$ is the vector containing r_i. Let $\mathbf{r}$ be subdivided into measured specific rate vector $\mathbf{r}_m$ and the other rate vector as $\mathbf{r}_c$. Then Equation 4.2 can be expressed as:

$$E\mathbf{r} = E_m\mathbf{r}_m + E_c\mathbf{r}_c = 0 \tag{4.3}$$

where E_m and E_c are the sub-matrices of E corresponding to $\mathbf{r}_m$ and $\mathbf{r}_c$, respectively. From Equation 4.3, r_c may be expressed as:

$$\mathbf{r}_c = -E_c^{-1}E_m\mathbf{r}_m \tag{4.4}$$

where E_c is assumed to be the square and non-singular. For example, consider the cultivation of yeast using glucose as a carbon source. The stoichiometric equation may be expressed as:

$$\underset{\text{Glucose}}{C_6H_{12}O_6} + O_2 + NH_3 \rightarrow \underset{\text{biomass}}{CH_{1.8}O_{0.5}N_{0.15}} + \underset{\text{ethanol}}{C_2H_5OH} + CO_2 + H_2O \tag{4.5}$$

where the stoichiometric balance with respect to C,H,O, and N may be expressed as:

$$\begin{array}{c} C \\ H \\ O \\ N \end{array}\begin{bmatrix} 6 & 0 & 0 & 1 & 1 & 2 & 0 \\ 12 & 0 & 3 & 1.8 & 0 & 6 & 2 \\ 6 & 2 & 0 & 0.5 & 2 & 1 & 1 \\ 0 & 0 & 1 & 0.15 & 0 & 0 & 0 \end{bmatrix}\begin{bmatrix} r_S \\ r_{O_2} \\ r_n \\ r_X \\ r_{CO_2} \\ r_e \\ r_w \end{bmatrix} = 0 \tag{4.6}$$

where the specific glucose consumption rate r_s, the specific oxygen consumption rate r_{O_2}, and the specific ammonia consumption rate r_n are negative, while the specific growth rate r_x, the specific CO_2 production rate r_{CO_2}, the specific ethanol production rate r_e, and the specific water formation rate r_w, are positive. Suppose that r_s, r_x, and r_{CO_2} can be measured, then the other specific rates can be estimated from Equation 4.4. Let E be subdivided and re-express the above equation as:

$$E_m\mathbf{r}_m + E_c\mathbf{r}_c = \begin{bmatrix} 6 & 1 & 1 \\ 12 & 0 & 1.8 \\ 6 & 2 & 0.5 \\ 0 & 0 & 0.15 \end{bmatrix}\begin{bmatrix} r_s \\ r_{CO_2} \\ r_x \end{bmatrix} + \begin{bmatrix} 0 & 0 & 2 & 0 \\ 0 & 3 & 6 & 2 \\ 2 & 0 & 1 & 1 \\ 0 & 1 & 0 & 0 \end{bmatrix}\begin{bmatrix} r_{O_2} \\ r_n \\ r_e \\ r_w \end{bmatrix} = 0 \tag{4.7}$$

Thus r_s, r_x, and r_{CO_2} can be used to estimate the other parameters by the following equation:

$$\begin{bmatrix} \hat{r}_{O_2} \\ \hat{r}_n \\ \hat{r}_e \\ \hat{r}_w \end{bmatrix} = - \begin{bmatrix} 3 & 1.5 & 0.4125 \\ 0 & 0 & 0.15 \\ 6 & 1 & 0.5 \\ -3 & -1.5 & -0.15 \end{bmatrix} \begin{bmatrix} r_S \\ r_{CO_2} \\ r_X \end{bmatrix} \tag{4.8}$$

Note that this equation is valid where ethanol (and CO_2) is assumed to be the sole metabolic product. When other metabolites, such as acetate, etc. are formed, the accuracy of the estimation based on the above equation will degrade.

Let us consider next the metabolic pathway equations. Let $\boldsymbol{A}$ be the metabolic stoichiometric coefficient matrix, $\boldsymbol{r}$ be the intracellular flux vector, and $\boldsymbol{q}$ be the extracellular measured specific rate vector, which include the specific substrate consumption rate, and the specific metabolite production rate, etc. Then the mass balance equation becomes:

$$\boldsymbol{Ar} = \boldsymbol{q} \tag{4.9}$$

where $\boldsymbol{A}$ is known by assuming the active metabolic network. If $\boldsymbol{q}$ is also known by measurement of all the specific rates, then the problem is to estimate $\boldsymbol{r}$ from the above equation. Since the A matrix is not necessarily square, multiply $\boldsymbol{A}^T$ from the left, and then multiply $(\boldsymbol{A}^T\boldsymbol{A})^{-1}$ from the left, and finally we have:

$$\boldsymbol{r} = (\boldsymbol{A}^T\boldsymbol{A})^{-1}\boldsymbol{A}^T\boldsymbol{q} \tag{4.10}$$

In practice, the following least square method is used:

$$\hat{r} = (\boldsymbol{A}^T\Sigma\boldsymbol{A})^{-1}\boldsymbol{A}^T\Sigma\boldsymbol{q} \tag{4.11}$$

where Σ is the variance-covariance matrix for the measurement error.

Consider another way of estimating the metabolic fluxes from the measured specific rates (Tsai and Lee, 1988). Let Equation 4.9 be expressed as:

$$\begin{bmatrix} q_m \\ q_c \end{bmatrix} = \begin{bmatrix} A_{11} & A_{12} \\ A_{21} & A_{22} \end{bmatrix} \begin{bmatrix} r_1 \\ r_2 \end{bmatrix} \tag{4.12}$$

where $\boldsymbol{q}_m$ is the measured specific rate, and q_c is the intracellular specific rate. Suppose A_{22} is the square matrix and non-singular. In general, we can set $\boldsymbol{q}_c$ to zero, and the above equation may be expressed as:

Published by Woodhead Publishing Limited, 2013

$$q_m = A_{11} r_1 + A_{12} r_2 \tag{4.13a}$$

$$0 = A_{21} r_1 + A_{22} r_2 \tag{4.13b}$$

The following equation may be derived from Equation 4.13b:

$$r_2 = -A_{22}^{-1} A_{21} r_1 \tag{4.14}$$

Substituting this into Equation 4.13a gives:

$$q_m = B r_1 \tag{4.15}$$

where

$$B \equiv A_{11} - A_{22}^{-1} A_{21} A_{12} \tag{4.16}$$

B is not necessarily the square matrix, and thus the least square estimate for $\mathbf{r}_1$ may be obtained from Equation 4.15 with Equation 4.16 as:

$$\hat{r}_1 = (B^T B)^{-1} B^T q_m \tag{4.17}$$

If the covariance matrix for measurement Σ is given, the least square estimate for $\mathbf{r}_1$ becomes:

$$\hat{r}_1 = [B^T \Sigma^{-1} B]^{-1} B^T \Sigma^{-1} q_m \tag{4.18}$$

Note that the following equation holds from Equation 4.14:

$$\hat{r}_2 = -A_{22}^{-1} A_{21} \hat{r}_1 \tag{4.19}$$

In the following, let us consider the metabolic flux analysis based on the above equations.

4.3 Application to photosynthetic bacteria

4.3.1 Background for microalgae cell

Microalgal cultures have received much attention in recent years because of their potential application for industrial CO_2 removal, production of many valuable metabolites, and life support in space (Borowitzke, 1988; Glombitza and Koch, 1989; Kurano and Miyachi, 1995). There have been several studies on the effects of medium composition, illumination intensity, and various photobio-reactors on the growth and photosynthetic rates of microalgae (Lee and Palsson, 1994; Mandanam and Palsson, 1998). In order to improve the performance of microalgal cultures, a deep understanding of the carbon and energy metabolism in microalgal cells is needed. In addition, an essential understanding of the metabolic

mechanism of microalgal cells may help to investigate the metabolism inside the plant cells, because there are many similarities between microalgae and plant cells. In fact, there are many distinct features about microalgal cell metabolism compared with other microorganisms. Microalgae can perform oxygenic photosynthesis and fix CO_2 through the Calvin cycle, like plant cells. That is, microalgal cells can trap light energy as the energy source and assimilate CO_2 as the carbon source. Moreover, organic substrates can also be utilized as carbon and energy sources by many microalgae (Droop, 1974). Therefore, by varying the nature of carbon and energy sources, the different underlying metabolic status of cells, especially the influence of light on carbon and energy metabolism, can be elucidated.

Here, metabolic flux analysis is considered to quantitatively assess intracellular fluxes through the main metabolic pathways of microalgal cells (Vallino and Stephanopulos, 1993; Bonarius et al., 1996). The performance of microalgal culture systems can be evaluated and compared through the efficiency with which the supplied energy to the culture can be utilized for biomass production (Tredici and Zittelli, 1998). In order to improve the energy utilization efficiency of the culture, we need a fundamental understanding of the energy conversion from the supplied energy to biomass formation, i.e. how the microalgal cells harvest light or chemical energy from the environment and then convert them into ATP, the universal currency of free energy for cell growth. The elucidation of carbon and energy metabolism of microalgae from metabolic flux distributions can provide a basis for the investigation of the energy utilization efficiency when cells are grown on different energy sources (Yang et al., 2000).

4.3.2 Metabolism of Chlorella cell

Consider the cultivation of *Chlorella pyrenoidosa* C-212, cultivated under autotrophic, mixotrophic, and cyclic light-autotrophic/dark-heterotrophic conditions (Yang et al., 2000). Metabolic flux analysis is used to clarify the metabolism of microalgae grown on different carbon and energy sources. Of particular interest is the effect of light on carbon and energy metabolism. Figure 4.1 shows the metabolic networks for autotrophic, heterotrophic, and mixotrophic cultures. The corresponding metabolic pathway reactions are listed in Tables 4.1 and 4.2 (Yang et al., 2000).

Algae cells can use light as their energy source. Light quanta absorbed by pigments drive the photosynthetic electron transport, which results in the reduction of $NADP^+$ and couples to the formation of ATP. It has been

Published by Woodhead Publishing Limited, 2013

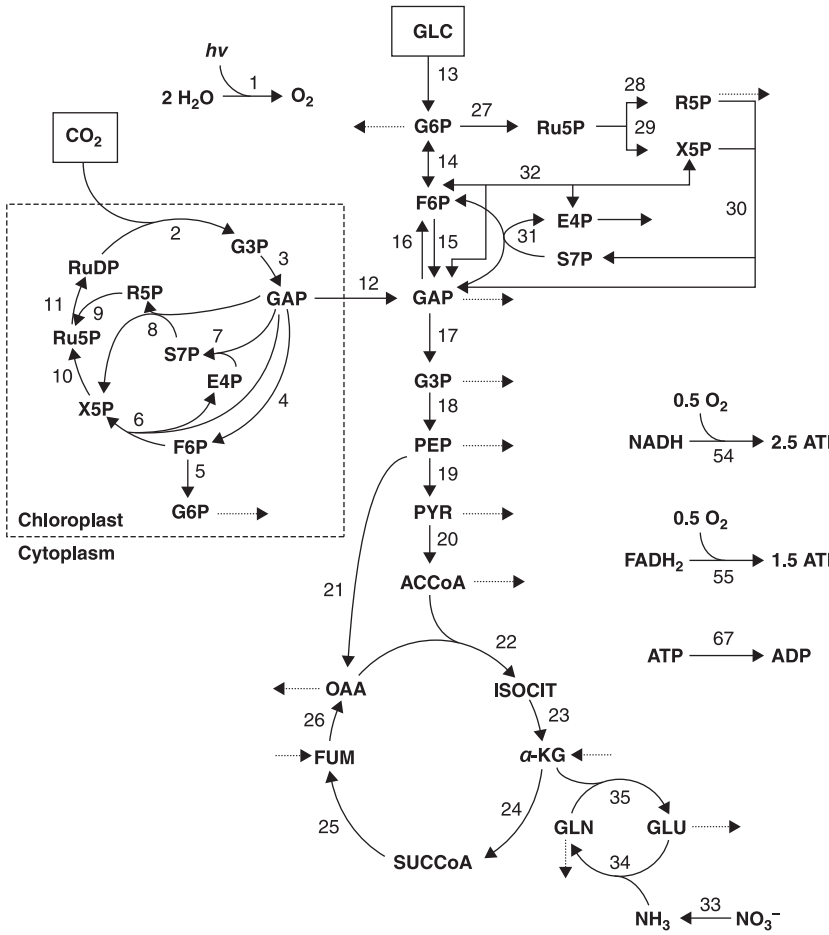

Figure 4.1 **Central reaction network for microalgae metabolism. Numbers correspond to the reactions shown in Tables 4.1 and 4.2. The dotted lines represent fluxes for cell synthesis**

reported that the P/2e$^-$ ratio (the number of ATP molecules formed per pair of electrons moving through the photosynthetic electron transport chain) is about 1.3 (Avron, 1989). According to the widely accepted two-step model of photosynthesis, 8 mol quanta of light are required to evolve 1 mol O_2. Therefore, the photosynthetic O_2 evolution rate can be determined from the photon flux absorbed. NADPH and ATP formed by the action of light reduce CO_2 by a series of dark reactions. The first step in the Calvin cycle, photosynthetic CO_2 fixation, is catalyzed by ribulose

1,5-bisphosphate carboxylase. This enzyme is also an oxygenase, which can react with O_2 and lead to a different pathway called photorespiration. Algae have the photorespiration pathway, and photosynthesis is inhibited by high O_2 concentration. However, under normal conditions, CO_2 loss by algal photorespiration is minimal (Tolbert, 1980). Here, the photorespiration pathway is not included in the metabolic network.

Photosynthesis reactions, including light reactions, the Calvin cycle, and starch synthesis, are located in chloroplasts. Glyceraldehyde 3-phosphate (GAP) is withdrawn from the Calvin cycle and exported to the cytoplasm for consumption. Although algae and plant cells have a high degree of sub-cellular compartmentation of metabolism, compartmentation of most metabolites between chloroplast, mitochondria, and cytoplasm is not considered because the extent to which biosynthetic reactions are localized in chloroplasts in algae cells is not understood or not yet fully established (Heldt and Flugge, 1987; Rees, 1987).

After the export of GAP from chloroplast to cytoplasm, the flow of carbon is divided into the synthesis of sugars or oxidation through the glycolytic pathway to pyruvate. Sugars, including sucrose, are the major storage products in the cytoplasm of plant cells. In addition, the structural carbohydrates, such as cell wall components, are considered to be synthesized in the cytoplasm. Some researchers found that the alga cell cultivated with [1-^{14}C] glucose yields starch in which glucose is still predominantly labeled in position 1 and the amount of glucose that remains unchanged is about 70% (Akazawa and Okakoto, 1980). This suggests that glucose can be directly converted to starch without prior conversion to GAP and then taken up by the chloroplast. Therefore, in the network of mixotrophic metabolism, one part of the exogenous glucose is directly converted to starch, and the remainder is oxidized through the glycolytic pathway.

In plant cells, replenishment of carbon to maintain the operation of the TCA cycle is achieved by anaplerotic reactions involving CO_2 fixation by Ppc (Wiskich, 1980). The pentose phosphate (PP) pathway has been reported to operate in the cytoplasm at the same time that the Calvin cycle is functioning in the chloroplast (Lloyde, 1974; Kelly and Latzko, 1980). In metabolic networks for autotrophic and mixotrophic cultures, only the PP pathway is considered to supply pentose phosphate for nucleic acid synthesis and produce E4P for the synthesis of shikimi acid, because the production of aromatic amino acids occurs in the cytoplasm and the transport of pentose phosphate out of the chloroplast is not possible. However, there is evidence that the PP pathway may function in both

Published by Woodhead Publishing Limited, 2013

cytoplasm and chloroplast in plant cells under dark condition (Graham, 1980). Therefore, both pathways located in different compartments are combined in the network of heterotrophic metabolism.

Nitrate is the predominant form of nitrogen available to most plants. Nitrate is reduced to ammonia before becoming available for assimilation. The reduction is divided into two steps: nitrate is reduced by a cytoplasmic NADH-dependent nitrate reductase to nitrite, which is further reduced to ammonia by a chloroplast-located NADPH-linked nitrite reductase (Morris, 1974). Glutamate dehydrogenase (GDH) and glutamine synthetase (GS) are considered as the important entries of ammonia into organic form. If both reactions are included in the metabolic network, a singularity arises. However, labeling experiments show the predominant operation of GS in algae cells (Miflin and Lea, 1980). Hence, only GS is included, and the glutamine formed provides the nitrogen donor to α-KG by the action of glutamate synthetase. GS/glutamate synthetase is considered in the reactions of ammonia assimilation in metabolic networks.

There are three different mechanisms of electron transport in the plant respiratory chain (Douce et al., 1987). De Gucht and van der Plas (1995) determined the activities of these pathways and calculated the P/O values for ATP production, which are about 2.5. Therefore, here it is assumed that the P/O ratios are 2.5 and 1.5 for NADH and $FADH_2$, respectively. It is not clear whether transhydrogenase, which catalyzes the reversible transfer of the hydride ion between NAD and NADP, is present in plant cells. Some experiments demonstrate the presence of this enzyme but with a very low activity, so this reaction can be disregarded in metabolic networks (Storey, 1980).

Of all the pigments, chlorophyll a takes a major fraction, thus only chlorophyll a formation is considered here. δ-Aminolevulinic acid (δ-ALA) is the key chlorophyll precursor molecule, which may be formed from different routes. The classical succinate-glycine pathway is the condensation of glycine and succinyl-CoA catalyzed by δ-ALA synthetase. In addition, 5-carbon compounds, glutamate, and α-KG are found to be incorporated into δ-ALA much more efficiently than are glycine and succinate in many green cells. Since the incorporation of all the synthesis reactions of δ-ALA in the metabolic network leads to a singularity and the C_5 route is a major contribution, this route can be considered to be the only contributor for δ-ALA formation (Castelfranco and Beale, 1981).

Eukaryotic algae and higher plants have a variety of lipids. Since these cells contain chloroplasts and have the biological function of photosynthesis, they have some unique lipids that are responsible for the

characteristic features of chloroplast membrane (Nichols, 1965). For metabolic flux analysis, all lipids but pigments may be lumped into diacylglycerol (DG), which is the key precursor in the synthesis of triglyceride, phospholipids, galactolipids, and perhaps sulfolipids. Although most of the synthesis reactions of fatty acids occur in the chloroplast, the source of AcCoA derives from its synthesis in the mitochondria. It should be pointed out that the fatty acid composition of the lipids isolated from *Chlorella* cells grown under different conditions varies considerably, particularly for the α-linolenic acid (C18:3) content (Wood, 1974). This leads to the difference in the synthetic reactions of DG in the three metabolic networks (Tables 4.1 and 4.2).

The protein composition may be obtained from Yanagi et al. (1995), and the composition of RNA and DNA is given in Wanka et al. (1970). The amino acid compositions of protein are assumed to be constant under different cultivation conditions, since the reported composition values for different cultivation conditions are similar (Fowden, 1962). The nucleotide compositions of DNA and RNA are also assumed to be maintained under different growth conditions. Three matrixes of stoichiometric coefficients are constructed using the reactions listed in Tables 4.1 and 4.2, and applied to calculate the metabolic fluxes under different culture conditions (Yang et al., 2000).

4.3.3 Cultivation of Clorella under different conditions

Figures 4.2–4.4 show the cell growth, the cellular composition, the consumption of glucose and nitrate, and the CO_2 production rate and O_2 uptake rates in autotrophic, mixotrophic, and cyclic light-autotrophic/

Table 4.1 Reactions in the networks of three different types of metabolism of *Chlorella* cell

Autotrophic network (CO_2 as a carbon source):
1, 2–11, 12, 14, 16–26, 27–32, 33–35, 36–53, 54–55, 56, 57, 60–62, 63, 66, 67
Heterotrophic network (glucose as a carbon source):
13–15, 17–26, 27–32, 33–35, 36–53, 54, 55, 57, 60–62, 64, 66, 67
Mixotrophic network (glucose and CO_2 as a carbon source):
1, 2–11, 12, 13–15, 17–26, 27–32, 33–35, 36–53, 54, 55, 57–62, 65–67

Published by Woodhead Publishing Limited, 2013

Table 4.2 Biochemical reactions for *Chlorella* cell

Light reactions

(4.1) $2H_2O+2NADP+2ADP+2Pi+0.125APF \Rightarrow 2NADPH+2H+2.6ATP+O_2$

Calvin cycle

(4.2) $H_2O+CO_2+RuDP \Rightarrow G3Pchl$

(4.3) $G3Pchl+ATP+NADPH+H \Rightarrow GAPchl+ADP+NADP+Pi$

(4.4) $2GAPchl+H_2O \Rightarrow F6Pchl+Pi$

(4.5) $F6Pchl \Leftrightarrow G6Pchl$

(4.6) $F6Pchl+GAPchl \Rightarrow X5Pchl+E4Pchl$

(4.7) $E4Pchl+GAPchl+H2O \Rightarrow S7Pchl+P_i$

(4.8) $S7Pchl+GAPchl \Rightarrow R5Pchl+X5Pchl$

(4.9) $R5Pchl \Rightarrow Ru5Pchl$

(4.10) $X5Pchl \Rightarrow Ru5Pchl$

(4.11) $Ru5Pchl+ATP \Rightarrow RuDP+ADP$

Transport of triose phosphate from chloroplast to cytoplasm

(4.12) $GAPchl \Rightarrow GAP$

Glycolytic pathway and tricarboxylic acid cycle

(4.13) $GLC+ATP \rightarrow G6P+ADP+H$

(4.14) $G6P \Leftrightarrow F6P$

(4.15) $F6P+ATP \rightarrow 2GAP+ADP+H$

(4.16) $2GAP+H_2O \Rightarrow F6P+P_i$

(4.17) $GAP+NAD+P_i+ADP \Leftrightarrow G3P+ATP+NADH+H$

(4.18) $G3P \Leftrightarrow PEP+H_2O$

(4.19) $PEP+ADP \Rightarrow PYR+ATP$

(4.20) $PYR+NAD+CoA \Rightarrow AcCoA+NADH+CO_2+H$

(4.21) $PEP+CO_2+ADP \Rightarrow OAA+ATP$

(4.22) $OAA+AcCoA+H2O \Leftrightarrow ISOCIT+CoA+H$

(4.23) $ISOCIT+NAD \Leftrightarrow AKG+NADH+CO_2$

(4.24) $AKG+CoA+NAD \Rightarrow SUCCoA+NADH+CO_2+H$

(4.25) $SUCCoA+ADP+Pi+FAD \Leftrightarrow FUM+FADH_2+ATP+CoA$

(4.26) $FUM+NAD+H_2O \Leftrightarrow OAA+NADH+H$

Pentose phosphate pathway

(4.27) $G6P+2NADP+H_2O \Rightarrow Ru5P+CO_2+2NADPH+2H$

(4.28) $Ru5P \Leftrightarrow R5P$

(*Continued*)

Table 4.2 Biochemical reactions for *Chlorella* cell (*Continued*)

(4.29) Ru5P⇔X5P

(4.30) R5P+X5P⇔S7P+GAP

(4.31) S7P+GAP⇔F6P+E4P

(4.32) X5P+E4P⇔F6P+GAP

Assimilation of nitrate

(4.33) NO3+NADH+3NADPH+5H⇒NH3+3NADP+NAD+3H_2O

(4.34) GLU+NH3+ATP⇒GLN+ADP+Pi

(4.35) AKG+NADPH+GLN⇒2GLU+NADP

Amino acid synthesis

(4.36) GLU+ATP+2NADPH+2H⇒PRO+ADP+Pi+H_2O+2NADP

(4.37) GLU+AcCoA+ASP+GLN+CO_2+NADPH+5ATP+3H2O⇒
ARG+AKG+CoA+AC+5ADP+FUM+5P_i+NADP+6H

(4.38) ASP+PYR+2NADPH+SUCCoA+GLU+ATP+2H⇒
LYS+SUC+AKG+CO_2+2NADP+CoA+ADP+Pi

(4.39) G3P+GLU+NAD+H_2O⇒SER+AKG+P_i+H+NADH

(4.40) SER+THF→GLY+METHF+H_2O

(4.41) SER+AcCoA+SO_4+4NADPH+4H+ATP⇒
CYS+AC+CoA+4NADP+ADP+3H_2O+P_i

(4.42) OAA+GLU⇒ASP+αKG

(4.43) ASP+GLN+2ATP+H_2O⇒ASN+GLU+2ADP+2P_i

(4.44) ASP+2ATP+2NADPH+H+H2O→THR+2ADP+2P_i+2NADP

(4.45) ASP+2NADPH+SUCCoA+CYS+MYTHF+ATP⇒
MET+CoA+SUC+PYR+NH3+ADP+Pi+THF+2NADP

(4.46) THR+PYR+NADPH+GLU+2H⇒ILE+NH_3+NADP+H_2O+CO_2+AKG

(4.47) PYR+GLU→ALA+AKG

(4.48) 2PYR+NADPH+2H+GLU⇒VAL+AKG+CO_2+NADP+H_2O

(4.49) 2PYR+NADPH+AcCoA+GLU+NAD+H_2O⇒
LEU+AKG+CoA+2CO_2+NADP+NADH

(4.50) 2PEP+E4P+NADPH+ATP+GLU+H⇒PHE+AKG+CO_2+H_2O+ADP+4Pi+NADP

(4.51) 2PEP+E4P+NADPH+ATP+GLU+NAD⇒
TYR+AKG+CO_2+NADH+ADP+4Pi+NADP

(4.52) 2PEP+E4P+NADPH+GLN+R5Pcyt+3ATP+SER⇒
TRP+6P_i+CO_2+GAP+GLU+2H+PYR+H_2O+3ADP+NADP

(4.53) R5P+6ATP+GLN+2NAD+ASP+FTHF⇒
HIS+AKG+FUM+2NADH+6ADP+7P_i+THF

Published by Woodhead Publishing Limited, 2013

Oxidative phosphorylation

(4.54) $NADH+0.5O_2+2.5ADP+2.5P_i+3.5H \Rightarrow 3.5H_2O+NAD+2.5ATP$

(4.55) $FADH_2+0.5O_2+1.5ADP+1.5P_i+2.5H \Rightarrow 2.5H_2O+FAD+1.5ATP$

Biosynthesis of macromolecules

(4.56) $G6P_{chl}+2ATP \Rightarrow STA$

(4.57) $G6P+2ATP \Rightarrow CAR$

(4.58) $G6P_{chl}+2ATP \Rightarrow 0.3STA$

(4.59) $G6P+2ATP \Rightarrow 0.7STA$

(4.60) $R5P+1.2ASP+2.1GLN+0.54GLY+1.1FTHF+0.54CO_2+8.2ATP+0.79NAD+2.2H_2O \Rightarrow RNA+2.1GLU+0.75FUM+1.1THF+8.2ADP+8.2P_i+0.79NADH+9.3H$

(4.61) $R5P+1.2ASP+0.25SER+2GLN+0.25GLY+FTHF+0.5CO_2+2.3H_2O+NADPH+0.76NAD+8ATP \Rightarrow DNA+0.75FUM+2GLU+THF+8ADP+8P_i+0.76NADH+NADP+9H$

(4.62) $0.09959ALA+0.0342ARG+0.02058ASN+0.04756ASP+0.01046CYS+0.05354GLU+0.02322GLN+0.08406GLY+0.0274HIS+0.02988ILE+0.07003LEU+0.05309LYS+0.01555MET+0.03176PHE+0.04268PRO+0.0193SER+0.04024THR+0.009932TRP+0.02583TYR+0.05044VAL+4ATP \Rightarrow PROT$

(4.63) $GAP+NADH+17AcCoA+33NADPH+34H+15ATP+3O_2 \Rightarrow DG+NAD+33NADP+15ADP+15P_i+17CoA+4H2O$

(4.64) $GAP+NADH+17AcCoA+32.4NADPH+34H+15ATP+2.2O_2 \Rightarrow DG+NAD+32NADP+15ADP+15Pi+17CoA+2.4H_2O$

(4.65) $GAP+NADH+17AcCoA+32.6NADPH+34H+15ATP+2.5O_2 \Rightarrow DG+NAD+33NADP+15ADP+15P_i+17CoA+2.7H2O$

(4.66) $8GLU+12AcCoA+21ATP+24NADPH+Mg_2{+}{+}MYTHF+3O_2 \Rightarrow CHLO+4NH_3+10CO_2+24NADP+THF+21ADP$

Miscellaneous reaction

(4.67) $ATP \Rightarrow ADP$

dark-heterotrophic cultures. It is assumed that the contents of RNA and DNA are maintained at 5.5 and 0.4% for all cultures (Nishimura et al., 1988). The experimental results for these cultures are summarized in Table 4.3. The autotrophic culture converts about 0.15 mol of CO_2 into biomass and evolves as much as 0.21 mol of O_2. Nevertheless, the increase in biomass results in a rapid reduction of the cell growth rate due to light limitation, hence the final cell concentration achieved by autotrophic growth is very low. With the increase in cell density, the contents of protein, lipids, and chlorophylls increase up to maximum values, then

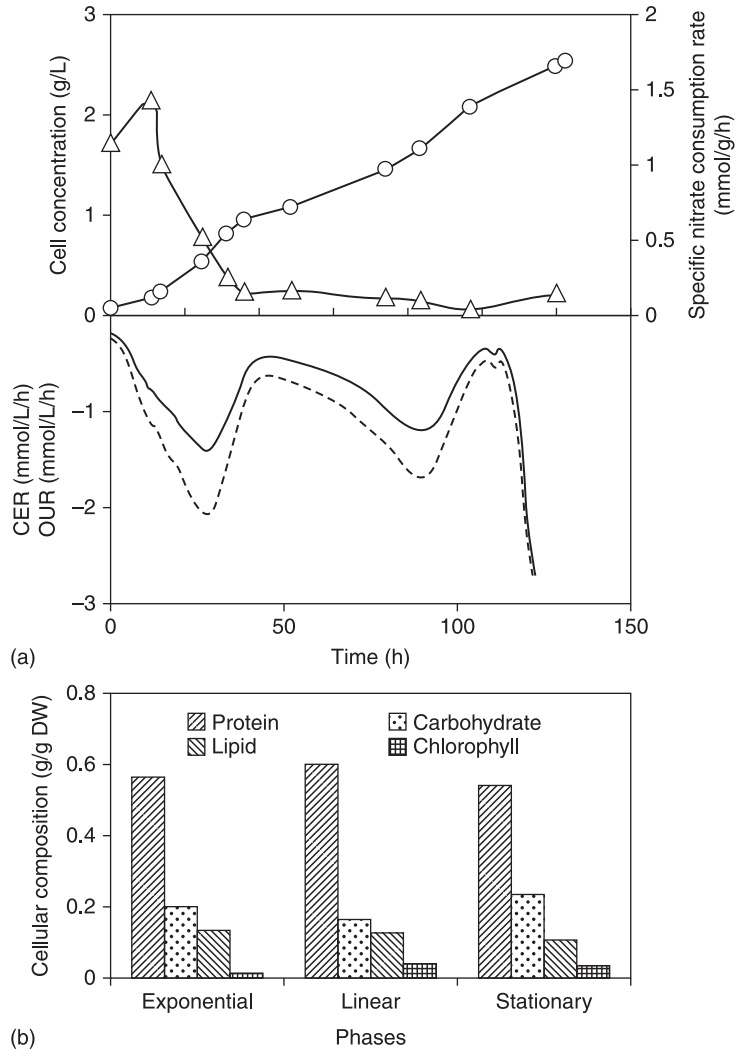

Figure 4.2 **Cultivation results of *C. pyrenoidosa* under autotrophic conditions: (a) Time profiles of cell growth (○), consumption of nitrate (△), rates of CO_2 production (solid line), and O_2 uptake (dotted line); (b) Contents of carbohydrates, protein, lipids, and chlorophylls in cells during the various growth phases. The incident light intensity was 500 μmol/m^2/s. The various growth phases were identified from the curve of cell growth: exponential phase (0–48 h), linear phase (48–120 h) and stationary phase (120 h–end)**

Published by Woodhead Publishing Limited, 2013

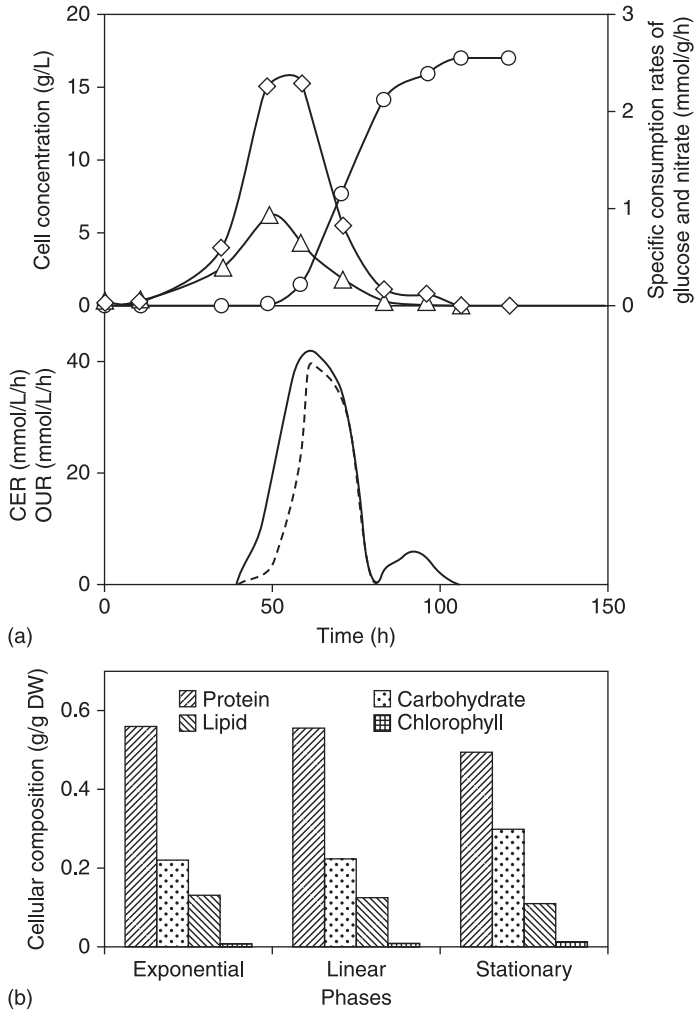

Figure 4.3 Cultivation results of *C. pyrenoidosa* under mixotrophic conditions: (a) Time profiles of cell growth (○), consumption of glucose (◇) and nitrate (△), and the rates of CO_2 production (solid line) and O_2 uptake (dotted line); (b) Contents of carbohydrates, protein, lipids, and chlorophylls in cells during the various growth phases. The light intensity was 500 μmol/m^2/s. Glucose was added to the culture and glucose concentration in the medium was controlled at 5 g/l. The various growth phases were identified from the curve of cell growth: exponential phase (0–58 h), linear phase (58–83 h), and stationary phase (83 h–end)

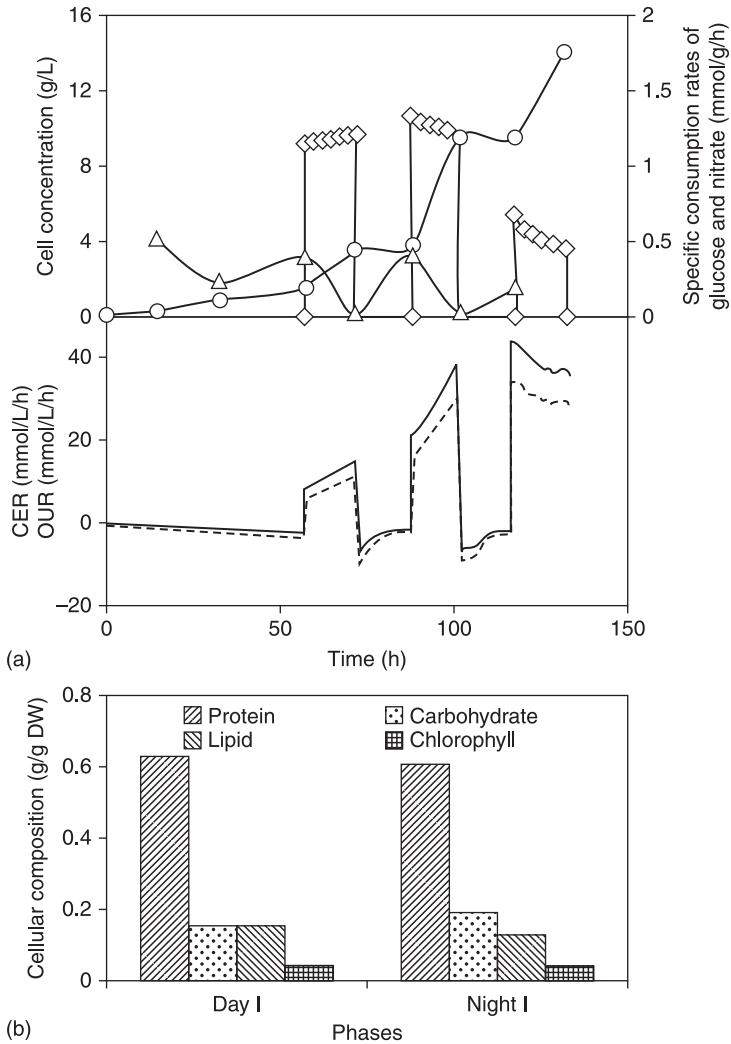

Figure 4.4 Cultivation results of *C. pyrenoidosa* under cyclic light-autotrophic/dark-heterotrophic conditions: (a) Time profiles of cell growth (○), consumption of glucose (◇) and nitrate (△), and the rates of CO_2 production (solid line) and O_2 uptake (dotted line); (b) Contents of carbohydrates, protein, lipids, and chlorophylls in cells during the first light/dark cycle. Cells were cultivated autotrophically for 24 h and then subjected to 12 h-light/12 h-dark cycles. The light intensity during the light period was 500 μmol/m^2/s. Glucose was added during the dark period and glucose concentration in the medium was controlled at 5 g/l

Published by Woodhead Publishing Limited, 2013

Table 4.3 The consumption of glucose, CO_2 production, and O_2 uptake of *C. pyrenoidosa* under different cultivation conditions

Experiment	$Y_{GLC/X}$ (mol/g)	$Y_{CO_2/X}$ (mol/g)	$Y_{O_2/X}$ (mol/g)
Autotrophic cultivation	–	−0.0398	−0.0556
Mixotrophic cultivation	0.0179	0.0653	0.0478
Cyclic cultivation	0.0170	0.0585	0.0384

decline gradually in the stationary growth phase, while the amount of carbohydrates decreases to the minimum value, and then accumulates to a high level. This result is in agreement with the variation of cellular ultra-structure, as reported by Hu et al. (1998), who suggest that this modification is characteristic of photo-adaption, so as to optimize light harvesting and light utilization.

As expected for mixotrophic and cyclic cultures, a significant improvement is observed in the biomass concentration, because the ability of *Chlorella* to grow on organic carbon sources is exploited in both cultures. However, the uptake of glucose also results in the consumption of O_2 and evolution of CO_2. The growth yields on glucose in the mixotrophic and cyclic cultures are close to each other. With light and organic carbon provided simultaneously as energy sources, the mixotrophic culture reaches the maximum final cell concentration, but forms a much smaller content of chlorophyll in comparison to the autotrophic culture. From the time profiles of the cyclic culture, it is found that the subsequent light autotrophic cell growth is not adversely affected by the carbon source addition during the night, showing that *Chlorella* cells can swiftly switch from autotrophic to heterotrophic metabolism and vice versa (Yang et al., 2000).

4.3.4 Metabolic flux distribution for different culture condition

By cultivating cells under autotrophic, mixotrophic, and cyclic autotrophic-heterotrophic cultures, it is possible to create different conditions for analyzing cell metabolism. Let us consider metabolic flux analysis to elucidate three different metabolisms. Before flux analysis, the data can be analyzed for the presence of measurement errors using elemental balances (Wang and Stephanopoulos, 1983). It can be shown

that the elemental balances for C and N can be closed and that no gross measurement errors are present. Therefore, a flux analysis can be carried out using the data given in Figures 4.2–4.4. Figure 4.5 shows the estimated fluxes for autotrophic, heterotrophic, and mixotrophic cultures (Yang et al., 2000). These values represent the flux distributions of the exponential growth phase during autotrophic and mixotrophic cultivations and the first dark period during the cyclic autotrophic/heterotrophic cultivation. The specific growth rates are almost the same for all three systems. The flux values are expressed in mmol produced metabolites per gram cell per unit time (mmol/g/h).

4.3.5 Effect of light on respiratory metabolism

The cells obtain substrates, reducing power, and ATP for biosynthesis through respiratory pathways, i.e. glycolysis, the PP pathway, and the TCA cycle linked to mitochondrial oxidative electron transport pathways. However, since the light reactions of photosynthesis can provide much reducing power and ATP, respiratory metabolism is unlikely to be essential for these normal functions. It has been proposed by some researchers that the respiratory activity of plants is inhibited in the light, while another indicates little or no effect of light on the respiratory rate (Kelly and Latzko, 1980). Thus the physiological evidence for the effect of light on respiratory metabolism in algae and plant cells is conflicting. Here the autotrophic flux distribution estimated from metabolic flux analysis can be assessed for the respiratory activity of microalgae in the light.

As shown in Figure 4.5, the autotrophic culture shows comparable activities of the glycolytic pathway and the TCA cycle with the heterotrophic culture. This result is consistent with the labeling experiments by Gibbs' laboratory using the alga *Scenedesmus*, which shows that the rates of equilibration of ^{14}C through the intermediates of the TCA cycle are essentially equivalent in light and dark (Kelly and Latzko, 1980). In addition, a significant flux through Ppc is observed for all cultures, suggesting the important role of this enzyme in maintaining the operation of the TCA cycle.

It is found in different plant cells that the percentage of glucose metabolism via the PP pathway is relatively small, i.e. between 5% and 15%, as compared to the total glycolytic flux (Rees, 1980). However, using mass balance to determine the flux distribution of algal cells in heterotrophic culture, the result indicates much higher activity in the PP

Published by Woodhead Publishing Limited, 2013

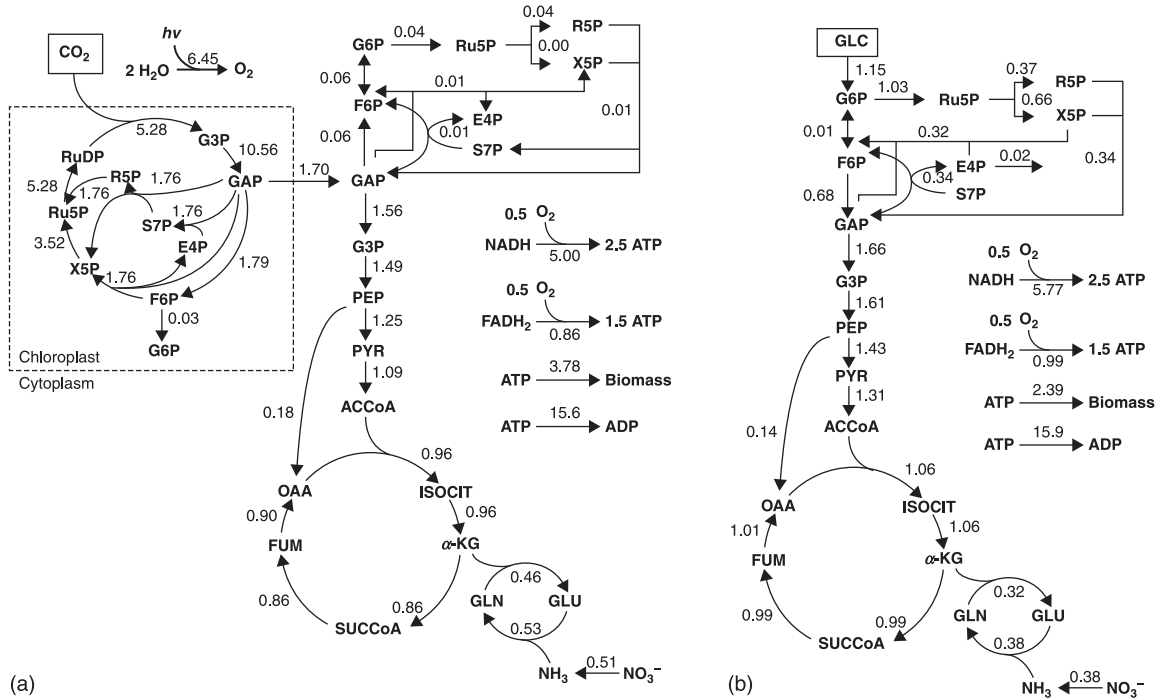

Figure 4.5 Metabolic flux distribution of *Chlorella* cells in: (a) autotrophic; (b) heterotrophic; and

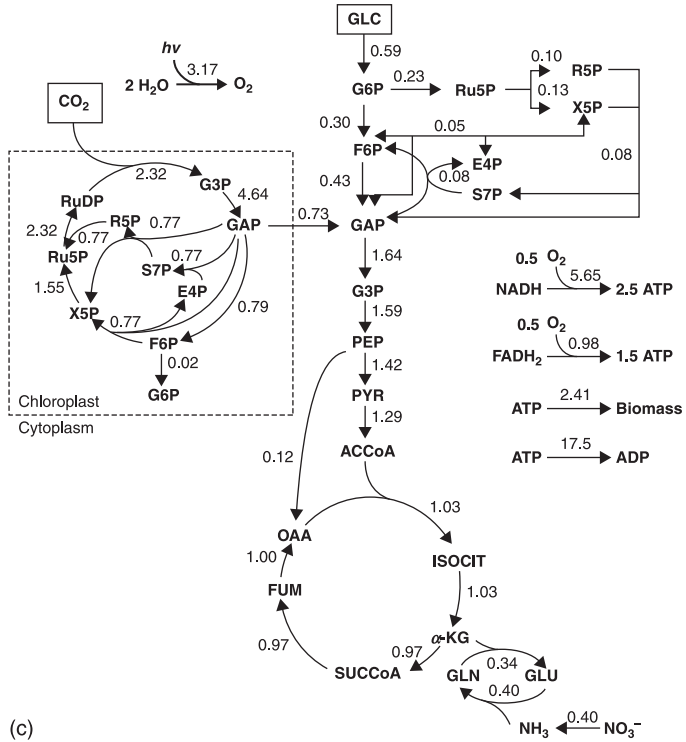

Figure 4.5 (C*ontinued*) (c) mixotrophic cultures. The flux values are expressed in mmol/g/h. These values represent the flux distributions of the exponential growth phase during the autotrophic (11 h) and mixotrophic (35 h) cultivations and the first dark period during the cyclic autotrophic/heterotrophic cultivation (48 h). The specific growth rates for all three systems are approximately 0.066 h^{-1}

pathway than found by others: about 90% of the glucose proceeds via G6PDH.

In the flux distribution under autotrophic condition, the flux through the PP pathway is very small. Since the function of NADPH synthesis is provided by photosynthetic electron transport, the main synthetic functions of the PP pathway in the light appear to be only the supply of precursors for synthesis of nucleic acid and amino acids. G6PDH is known as the major site for regulation in the PP pathway, and its activity is strongly inhibited by NADPH (Turner et al., 1980). It has already been proposed that the light-modulated regulation of G6PDH may be due to a change in the ratio of NADPH/$NADP^+$ (Copeland and Turner, 1987). The low activity of the PP pathway in the autotrophic culture is therefore probably a result of light-mediated control on G6PDH.

It has been suggested that the mitochondrial electron transport will be light-inhibited because of the high ATP/ADP ratios in the light (Kelly and Latzko, 1980). However, other data indicate that any increase in the cytoplasmic ATP/ADP ratios observed in photosynthetic cells upon light to dark transitions is only transient and that steady-state cytoplasmic ATP/ADP ratios are similar under both light and dark conditions (Raymond et al., 1987). Furthermore, it has been shown that light has no direct effect on the activity of the respiratory chain in green algae and plant cells (Dry et al., 1987). It seems that the function of mitochondrial electron transport may have been underestimated and that oxidative phosphorylation can provide a significant fraction of energy for cell growth.

4.3.6 Energy metabolism of microalgae under different culture condition

From the estimated flux distribution, the fluxes involved in the generation and utilization of ATP can be obtained (Table 4.4). Under autotrophic condition, a significant fraction (40%) of ATP is formed from mitochondrial oxidative phosphorylation, suggesting its important role in ATP production. The Calvin cycle is the main ATP sink in the autotrophic culture, and the ATP demand for the assimilation of CO_2 accounts for about 77% of the total. From Table 4.4, the theoretical yields of biomass on ATP for three different cultures can be calculated (Table 4.5), where these values are comparable to the yield found in plant and microbial systems (de Gucht and van der Plas, 1995; Aristidou et al., 1999). Obviously, the ATP yield decreases in the following order:

Table 4.4 The generation and utilization of ATP in the autotrophic, heterotrophic, and mixotrophic cultures

Autotrophic culture		Heterotrophic culture		Mixotrophic culture	
ATP production					
Direct ATP	3.83	Direct ATP	3.54	Direct ATP	3.70
Oxidative phosphorylation	13.8	Oxidative phosphorylation	15.9	Oxidative phosphorylation	15.5
Photo-phosphorylation	16.8			Photo-phosphorylation	8.24
ATP consumption					
Calvin cycle	15.8	Glucose uptake	1.15	Glucose uptake	0.59
Synthesis of cell mass	3.78	Synthesis of cell mass	2.39	Synthesis of cell mass	2.41
				Calvin cycle	6.96

heterotroph > mixotroph > autotroph. Since the Calvin cycle requires a large amount of ATP, the difference in the contribution of the Calvin cycle to total carbon metabolism leads to the different ATP yields. From the flux of excess ATP, the growth-related maintenance ATP requirements can be estimated (Table 4.5). It can be seen that a significant amount of available ATP is required for maintenance. Maintenance processes take up as much as 45–82% of the total ATP produced. This result is consistent with the data reported by de Gucht and van der Plas (1995), who found that maintenance processes require 50–75% of the available ATP in the continuous cultures of plant cells. This maintenance energy includes ATP requirements for transport, translocation, futile cycles, and so on. Especially for algae and plant cells, which have a high degree of subcellular

Table 4.5 Theoretical yields of biomass on ATP and ATP maintenance requirements in the autotrophic, heterotrophic, and mixotrophic cultures

Culture	Theoretical ATP yield (g/mol)	ATP maintenance demand (mmol/g/h)
Autotrophic culture	3.11	15.6
Heterotrophic culture	19.3	15.9
Mixotrophic culture	6.64	17.5

Published by Woodhead Publishing Limited, 2013

compartmentation of metabolism, various transport reactions are involved in the metabolic pathways (Rees, 1987). These transport processes may consume a large amount of energy.

In autotrophic and heterotrophic cultures, there are only two energy contributors: light or glucose. However, both light and glucose are sources for ATP production in the mixotrophic culture. Since GAP generated by photosynthesis partly enters the glycolytic pathway and the TCA cycle, both light and glucose account for the production of NADH and $FADH_2$ in the TCA cycle. Therefore, ATP production from light includes not only ATP produced from photophosphorylation but also ATP provided by the oxidative phosphorylation of NADH and $FADH_2$ derived from photosynthesis. The contribution of light and glucose to NADH and $FADH_2$ can be calculated using the fractional contribution model (Xie and Wang, 1996). With this information, the contribution of light and glucose to ATP production can be obtained (Table 4.6). The amount of ATP produced from photosynthesis is about 63%. Hence, light is the major source for ATP production in the early phase of mixotrophic cultivation.

4.3.7 Energy conversion under different culture condition

In all three cases, the energy provided by light and/or glucose is absorbed by the microalgal cells, then transformed into ATP for various energy demands inside the cells. Thus the conversion of energy involves three energy forms, the energy supplied to the culture, the energy absorbed by the cells, and the high free energy stored in the phosphoanhydride bonds of ATP. Figure 4.6 shows the conversion efficiencies among the three energy forms in autotrophic, heterotrophic, and mixotrophic cultures. Since the concentration of the organic substrate is maintained as constant, the energy provided by the addition of glucose is completely utilized by

Table 4.6 Contributions of light energy and glucose to ATP production in the exponential phase of mixotrophic cultures

Energy source	ATP production	
	mmol/g/h	%
Light	17.3	63.1
Glucose	10.1	36.9

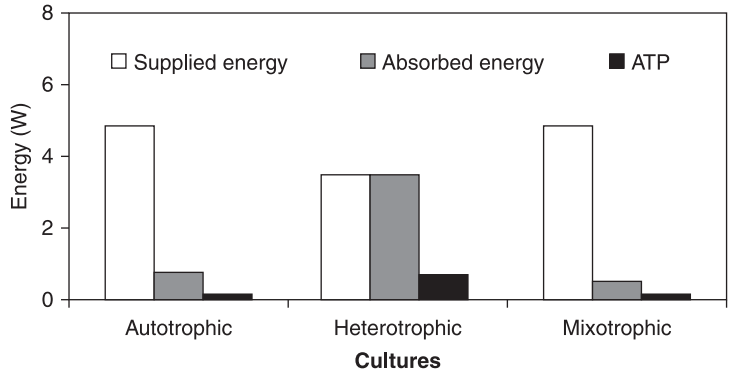

Figure 4.6 **Energy conversion efficiency between the energy supplied to the culture, the energy absorbed by the cells, and the high free energy stored in ATP. These values represent the energy conversion efficiency of the exponential growth phase during the autotrophic and mixotrophic cultivations and the first dark period during the cyclic autotrophic/heterotrophic cultivation. The supplied and absorbed light energy were calculated from the appropriate equations (Grima et al., 1997), and the estimation of the total ATP produced was based on the flux distribution shown in Figure 4.5. Assuming that the wavelength of fluorescent light is 600 nm, 1 mol of photons has an energy content of 200.8 kJ. The supplied glucose energy was calculated by multiplying the glucose consumption rate by the free energy change in the reaction of glucose oxidation (2868.852 J/mol). The free energy stored in 1 mol ATP is 30.5 kJ**

the cells under heterotrophic and mixotrophic conditions. The capture of light energy in the autotrophic culture is found to be as low as 14% of the total supplied light energy, while in the mixotrophic culture, for which both light and glucose provide energy, the conversion efficiency of the supplied energy to the absorbed energy is even lower than that of the autotrophic culture. The low energy availability in the mixotrophic culture is the result of a lower pigment content in the cells.

From Figure 4.6, microalgal cells transfer 10, 18, and 12% of the absorbed energy into ATP in the autotrophic, heterotrophic, and mixotrophic cultures, respectively. The maximum thermodynamic

Published by Woodhead Publishing Limited, 2013

efficiency of ATP formation from the absorbed energy can be calculated from the fluxes through the relevant metabolic networks at zero growth rates (Figure 4.7). This figure shows that the theoretical yield of ATP on the absorbed energy, Y_{ATP}/AE_{max}, is highest in the heterotrophic culture, while maximum ATP production in the autotrophic culture is only 16% of the harvested light energy. In the mixotrophic culture, Y_{ATP}/AE_{max} is a linear function of the fraction of absorbed light energy of the total. Since the mitochondrial oxidative phosphorylation is a more efficient energy-producing pathway than the photophosphorylation, the conversion efficiency of ATP from the absorbed energy depends on the contributions of both phosphorylation systems to the total ATP production (Lee and Erickson, 1987). If the energy conversion efficiency through the photosynthetic electron transport can be improved, a higher availability of ATP from the absorbed energy will be expected. It has been reported that an algae that lacks photosystem I requires a single photon rather than two in the process of photosynthesis (Greenbaum et al., 1995). Therefore, the conversion efficiency of light energy into chemical energy can be potentially doubled (Yang et al., 2000).

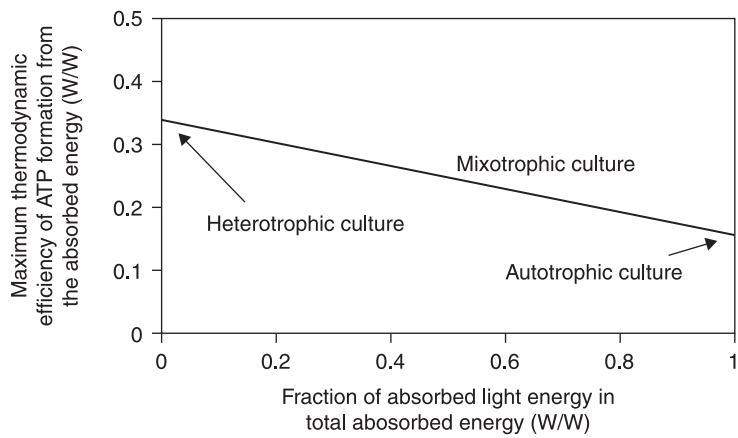

Figure 4.7 **Theoretical thermodynamic efficiency of ATP formation from the absorbed energy (Y_{ATP}/AE_{max}) as a linear function of the fraction of the absorbed light energy of the total. Y_{ATP}/AE_{max} was calculated from the fluxes through the relevant metabolic network at zero growth rate. For the fraction of the light energy of the total absorbed energy, 0 represents heterotrophic culture, and 1 represents autotrophic culture**

From the above analysis, about 18% of the supplied energy is transformed to ATP in the heterotrophic culture, while the percentages decrease to 1.5% and 1.1% in the autotrophic and mixotrophic cultures, respectively. Apparently, the difference is caused by the different energy sources supplied to the cultures. It seems that compared with the organic substrate, light energy is difficult to trap and convert to ATP by the cells.

4.3.8 Energy economy under different culture condition

The energy economy of microalgae cultures can be evaluated through the efficiency of energy utilization. Table 4.7 shows the overall yield of biomass on the supplied energy for the autotrophic, mixotrophic, and cyclic autotrophic/heterotrophic cultivations. Not surprisingly, the energetic growth yield in the autotrophic culture is lowest due to the inefficient conversion of light energy into biomass, as discussed above. For mixotrophic and cyclic autotrophic/heterotrophic cultures, both light and glucose are the energy sources. However, the difference in the energy supply results in different bioenergetic yields. The biomass energetic yield in the mixotrophic culture is lower than that in the cyclic culture.

The conversion efficiencies of total energy and light energy can be calculated for different growth phases during mixotrophic cultivation (Figure 4.8). Total ATP production and ATP derived from light can be estimated from metabolic fluxes. Figure 4.8 shows that in the exponential phases, where light plays a major role in ATP production, only 0.73% of the supplied light energy is transferred into ATP. This value is much lower than that in the autotrophic culture, because of pigment in the mixotrophic cells. The formation of photosynthetic apparatus is disturbed due to the

Table 4.7 Biomass yields on the supplied energy ($Y_{X/SE}$) in the autotrophic, mixotrophic, and cyclic autotrophic/heterotrophic culture experiments

Experiment	Cell produced (g)	Glucose supplied (kJ)	Light supplied (kJ)	$Y_{X/SE}$ (g/kJ)
Autotrophic culture	3.78	–	2144.6	0.00177
Mixotrophic culture	25.5	1307.6	2099.4	0.00749
Cyclic culture	21.1	1041.1	1238.6	0.00924

Published by Woodhead Publishing Limited, 2013

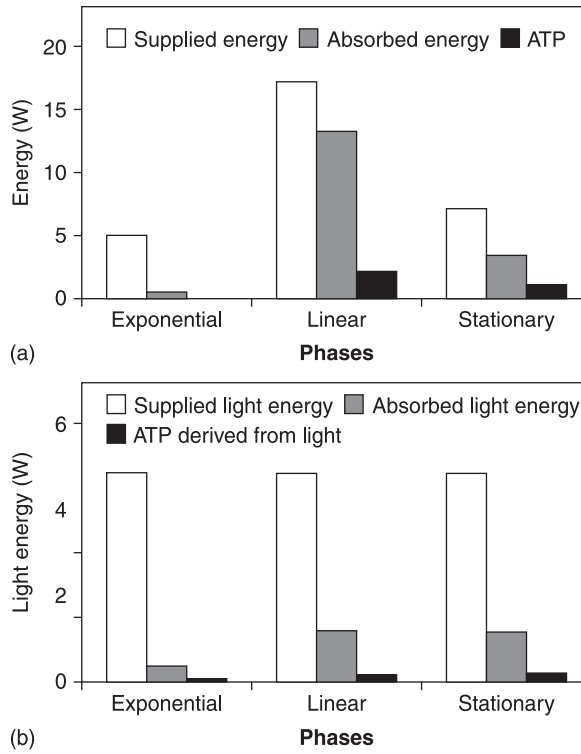

Figure 4.8 **Conversion efficiency of: (a) total energy; and (b) light energy during the various growth phases of the mixotrophic cultivation. The total ATP production and ATP derived from light were estimated from the results of metabolic flux analysis**

presence of the organic substrate. With the age of the culture and the increase in cell concentration, the contribution of light energy to ATP production is decreased according to flux analysis. In the linear phase, nearly all the ATP produced originated from glucose, and the light energy supplied to the culture cannot be efficiently utilized for cell growth due to high cell density. Therefore, energy is not utilized efficiently in the mixotrophic cultivation. This result is unexpected, since the mixotrophic culture is often applied for commercial algal production. It is expected that the two processes of photosynthesis and glucose catabolism proceed independently and do not interact with each other (Ogawa and Aiba, 1981). However, from the above analysis, it seems that the photosynthetic

capacity of microalgal cells is reduced significantly, due to the uptake of glucose (Yang et al., 2000).

Figure 4.9 shows the energy conversion efficiency between the three energy forms during the first light/dark cycle of the cyclic autotrophic/heterotrophic culture. In the cyclic culture, cells are cultivated autotrophically for the first two days, and then subjected to dark/light cycles. From Figure 4.9, during the first two days of autotrophic growth, the light energy absorbed by the cells has reached the maximum value, indicating that autotrophic growth had undergone a rapid growth phase and the availability of light to the culture has started to be limited. In the subsequent dark period, the addition of glucose to the culture enhanced cell growth and results in a significant increase in cell concentration. Therefore, the advantage of the cyclic culture is that autotrophic cell growth and photosynthetic processes are not adversely affected by the addition of organic substrate during the night. In the late light period of the cyclic culture, although the growth rates are very low, autotrophic growth can improve the contents of some important components, such as pigments and linolenic acid. Thus the nutritional value and product quality of the microalgae will be better than those in the simple heterotrophic culture. More importantly, the cyclic culture can be easily employed for the utilization of solar energy. As is well known, utilization of solar energy is very desirable, but the solar light supply is not continuous due to diurnal and seasonal changes (Ogbonna and Tanaka,

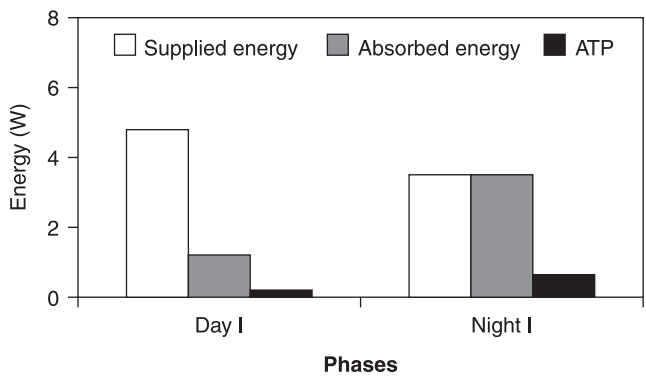

Figure 4.9 **Energy conversion efficiency between the three energy forms during the first light/dark cycle of the cyclic autotrophic/heterotrophic cultivation. The total ATP production and ATP derived from light were estimated from the results of metabolic flux analysis**

Published by Woodhead Publishing Limited, 2013

1996). For autotrophic and mixotrophic cultures, which require continuous illumination, it is necessary to capture and concentrate the solar energy for the light supply during the night, while for the illumination of the cyclic culture, solar light energy can be used directly. Therefore, from the viewpoint of economy, the cyclic light-autotrophic/dark-heterotrophic culture can be employed for efficient production of microalgae.

In summary, the metabolic flux distribution of microalgal cells for autotrophic, heterotrophic, and mixotrophic cultures, and the subsequent analysis indicate that the glycolytic pathway, the TCA cycle, and mitochondrial oxidative phosphorylation maintain high activity during illumination, implying little effect of light on these pathways. However, the flux through the PP pathway during illumination is very small due to light-mediated regulation. The theoretical yields of biomass on ATP and the maintenance ATP requirements can be estimated, and the results show that the difference in the contribution of the Calvin cycle to total carbon metabolism leads to different ATP yields of the three cultures, and a significant amount of the available ATP is required for maintenance processes in microalgal cells. The energy conversion efficiency between the energy supplied to culture, the energy absorbed by cells, and the free energy conserved in ATP can be calculated, and the heterotrophic culture generates more ATP from the supplied energy than the autotrophic and mixotrophic cultures. The maximum thermodynamic efficiency of ATP production from the absorbed energy (Y_{ATP}/AE_{max}), which is calculated from the metabolic fluxes at zero growth rate, is the highest in the heterotrophic culture and as low as 16% in the autotrophic culture. In the mixotrophic culture, Y_{ATP}/AE_{max} is a linear function of the fraction of absorbed light energy of the total. The biomass yield on the supplied energy is lowest in the autotrophic cultivation, and the cyclic culture displays the most efficient utilization of energy for biomass production. The analysis of the energy utilization efficiency may be useful for providing information concerning cell energetics and guidance to improve microalgal cell culture performance (Yang et al., 2000).

4.4 Metabolic flux analysis of a single gene knockout *E. coli* under anaerobic conditions

Although the conventional metabolic flux analysis has some limitations, as stated in the introduction, this may be applied to anaerobic culture,

since the metabolic pathway network does not include cyclic pathways or closed loops, and the reaction mainly occurs unidirectionally. Here we consider the metabolic flux analysis for several single-gene knockout *E. coli* cultivated under anaerobic condition. Before metabolic flux analysis, let us consider the fermentation characteristics (Table 4.8) and some enzyme activities for *pflA*, *pta*, *ppc*, *adhE*, and *pykF* mutants, as compared to the wild type BW25113 (Table 4.9) (Zhu and Shimizu, 2005). The *pflA* mutant shows much higher activity of GAPDH, LDH, Ppc, and Ack, as compared to the parent strain. The up-regulation of GAPDH and LDH implies the coupling between the NADH production and consumption between the two corresponding reactions. The specific Pyk activity of the *pflA* mutant is higher than that of the parent strain. Since ATP can only be produced through substrate level phosphorylation in glycolysis and the Pta–Ack pathway, the up-regulation of the enzyme activity of Pyk and Ack implies ATP requirement for the cell. Similarly to the *pflA* mutant, the simultaneous up-regulation of GAPDH and LDH is also observed in the *pta* mutant (Table 4.9). Interestingly, Pfl is inactivated in this mutant, which implies a common regulatory mechanism that controls the expressions of *pta* and *pfl* genes. The significant difference between *pta* and *pflA* mutants is the specific activity of Ppc. In the *pta* mutant, this enzyme activity changes little compared to the parent strain. However, the *pta* mutant produces more succinate than the *pflA* mutant, despite lower Ppc activity (Table 4.9), which implies that the intracellular pool size of PEP plays another important role in the metabolic regulation.

The enzyme activity of Ack and ADH, both of which are the AcCoA assimilation pathway enzymes, increases in the *ppc* mutant. However, the enzyme activity of Pfl, which supplies AcCoA for these two reactions, is much lower than that of the parent strain (Table 4.9). Less acetate and ethanol are produced in the *ppc* mutant than those of the parent strain. Although the activity of LDH is lower, lactate production is higher in the *ppc* mutant compared to that of the parent strain. The activity of Pyk in the *ppc* mutant is about one-quarter of that in the parent strain. Pyk activity in the *adhE* mutant is also down-regulated. The activity of Ack is higher in these two strains and the *pykF* mutant, which may be due to ATP generation under anaerobic condition. The activities of LDH and Pfl are both down-regulated in the *adhE* mutant, which is consistent with relatively lower lactate and formate yield in this strain (Table 4.8). The *pykF* mutant shows higher Ppc activity, while the activities of LDH and ADH are both down-regulated as compared to the parent strain (Zhu and Shimizu, 2005).

Published by Woodhead Publishing Limited, 2013

Table 4.8 Comparison of fermentation results

Strain	Specific growth rate μ (h^{-1})	Yield on glucose (g/g)%						
		Biomass	Lactate	Acetate	Formate	Succinate	Ethanol	Pyruvate
Wild	0.85±0.08	30.1±0.	1.2±0.0	24.3±0.1	30.0±0.2	5.0±0.2	14.7±0.3	0.2±0.0
Δ*Pfl*A	0.18±0.04	8.1±0.1	72.5±0.0	1.1±0.1	0.0±0.2	0.0±0.0	1.0±0.0	1.1±0.0
Δ*pta*	0.24±0.04	6.9±0.1	51.3±0.0	1.6±0.1	2.1±0.2	4.5±0.1	0.0±0.0	0.0±0.0
Δ*ppc*	0.01±0.02	4.6±0.1	32.2±0.0	13.5±0.1	9.4±0.2	0.3±0.0	6.2±0.1	4.6±0.0
Δ*adh*E	0.03±0.02	11.4±0.1	9.7±0.0	42.4±0.1	12.1±0.2	3.2±0.1	0.2±0.0	0.0±0.0
Δ*pyk*F	0.48±0.05	13.0±0.1	2.1±0.0	34.0±0.1	22.9±0.2	6.9±0.2	12.0±0.2	0.0±0.0

Table 4.9 Comparison of enzyme activities

	Enzyme activities (mmol/min mg protein)								
	G6PDH	6PGDH	GAPDH	Pyk	LDH	Ppc	Pfl	Ack	ADH
wild	0.152±0.023	0.18±0.002	0.008±0.001	0.657±0.102	0.503±0.120	0.008±0.003	0.071±0.012	0.038±0.006	0.006±0.000
Δ*pfl*A	0.252±0.061	0.079±0.010	0.076±0.011	0.726±0.170	2.093±0.512	0.343±0.122	0.004±0.004	4.088±0.200	0.011±0.002
Δ*pta*	0.187±0.027	0.001±0.001	0.060±0.008	0.512±0.006	1.621±0.306	0.005±0.001	0.013±0.001	3.465±0.195	0.005±0.001
Δ*ppc*	0.017±0.002	0.000±0.000	0.014±0.001	0.183±0.060	0.164±0.020	0.003±0.002	0.025±0.006	0.629±0.035	0.040±0.009
Δ*adh*E	0.013±0.002	0.004±0.001	0.008±0.003	0.108±0.021	0.000±0.000	0.005±0.001	0.043±0.001	0.536±0.035	0.000±0.000
Δ*pyk*F	0.052±0.006	0.017±0.003	0.020±0.005	0.009±0.003	0.069±0.030	0.013±0.001	0.050±0.004	0.293±0.016	0.001±0.001

Let us consider how the intracellular metabolite concentrations change in response to specific-gene knockout (Table 4.10). The pool sizes of G6P, FDP, and PYR increase 3.5 to 20 times in the *pflA* mutant, as compared to the parent strain. The PEP concentration is lower in the *pflA* mutant. The low PEP concentration causes less succinate production, even with high Ppc activity. The metabolite concentrations in the *pta* mutant are similar to those in the *pflA* mutant, except for significantly accumulated PEP. In the case of the *pykF* mutant, all intracellular metabolites in glycolysis are significantly accumulated, as compared to the parent strain and other mutants. Two of the lactate producing strains, such as *pflA* and *pta* mutants, show a higher NADH/NAD^+ ratio as compared to the parent strain. Therefore, it is reasonable to consider that lactate production is promoted by intracellular redox balance pressure in these two strains. The value of ATP /AXP (ATP+ADP+AMP) is less in the mutants as compared to the parent strain, and this ratio is low in *pta* and *pykF* mutants (Zhu and Shimizu, 2005).

Consider the intracellular metabolic flux distribution estimated, as stated in Section 4.2, for each strain using the fermentation data during the exponential growth phase. Based on the biochemistry framework (Figure 4.10), the constraints imposed by the stoichiometry and the measured specific rates during the exponential phase can be used to obtain the flux distribution. The flux values are shown in Table 4.11. Although one of the catabolic pathways is blocked by gene knockout, the higher glucose uptake rate (v_1), followed by higher glycolytic flux, may be seen in such strains as *pflA*, *pta*, and *pykF* mutants, as compared to the parent strain. In particular, the glucose uptake rate is about 40% higher in the *pykF* mutant than that in *E. coli* BW25113. This is consistent with the significantly higher intracellular concentration levels of the glycolytic metabolites in the *pykF* mutant. The flux through GAPDH (v_3) is shown to be regulated by the intracellular NADH/NAD^+ ratio (Garrigues et al., 1997; De Graef et al., 1999). It has been shown that NADH competitively combines with GAPDH and inhibits the reaction through this enzyme. The GAPDH activity in the mutant strains, such as *pflA*, *pta*, and *pykF* mutants, are 9.5-fold, 7.5-fold, and 2.5-fold of that in the parent strain, respectively (Table 4.9). The intracellular NADH/NAD^+ ratio is significantly lower in the *pykF* mutant (Table 4.10) and, therefore, the higher glycolysis flux is not restricted by the competitive inhibition of NADH on the reaction through relatively high levels of GAPDH. While the intracellular NADH/NAD^+ ratio is significantly higher in *pflA* and *pta* mutants than the other strains, lactate is produced in these two mutants to regenerate NAD^+ needed for

Published by Woodhead Publishing Limited, 2013

Table 4.10 Comparison of intracellular metabolite concentrations in *E. coli* mutants

	Metabolite concentration (mM/g DCW)											
	G6P	FDP	PEP	PYR	AcCoA	ATP	ADP	AMP	ATP/AXP	NADH	NAD	NADH/NAD
BW25113	0.05±0.01	4.59±0.02	0.32±0.12	8.21±0.01	0.07±0.00	3.06±0.17	0.38±0.01	0.21±0.01	0.84	0.018±0.002	0.143±0.001	0.126
Δ*pflA*	1.09±0.01	16.41±0.11	0.12±0.04	25.49±0.01	0.05±0.00	1.69±0.11	0.20±0.01	0.20±0.01	0.81	0.056±0.001	0.060±0.002	0.933
Δ*pta*	0.54±0.03	15.08±0.03	1.27±0.20	21.83±0.55	0.01±0.00	1.82±0.16	1.17±0.08	1.12±0.17	0.44	0.047±0.001	0.129±0.007	0.680
Δ*ppc*	0.84±0.03	24.46±0.04	0.96±0.07	38.72±2.26	0.05±0.02	4.19±0.07	3.71±1.14	1.16±0.43	0.53	0.018±0.004	0.170±0.010	0.106
Δ*adhE*	0.32±0.01	11.41±0.03	0.46±0.08	18.40±0.25	0.01±0.00	1.38±0.04	0.69±0.02	0.46±0.04	0.55	0.010±0.006	0.058±0.009	0.167
Δ*pykF*	1.15±0.02	30.90±0.90	3.67±0.06	46.96±1.98	0.08±0.02	2.65±0.10	2.27±0.05	1.01±0.08	0.47	0.002±0.005	0.177±0.008	0.010

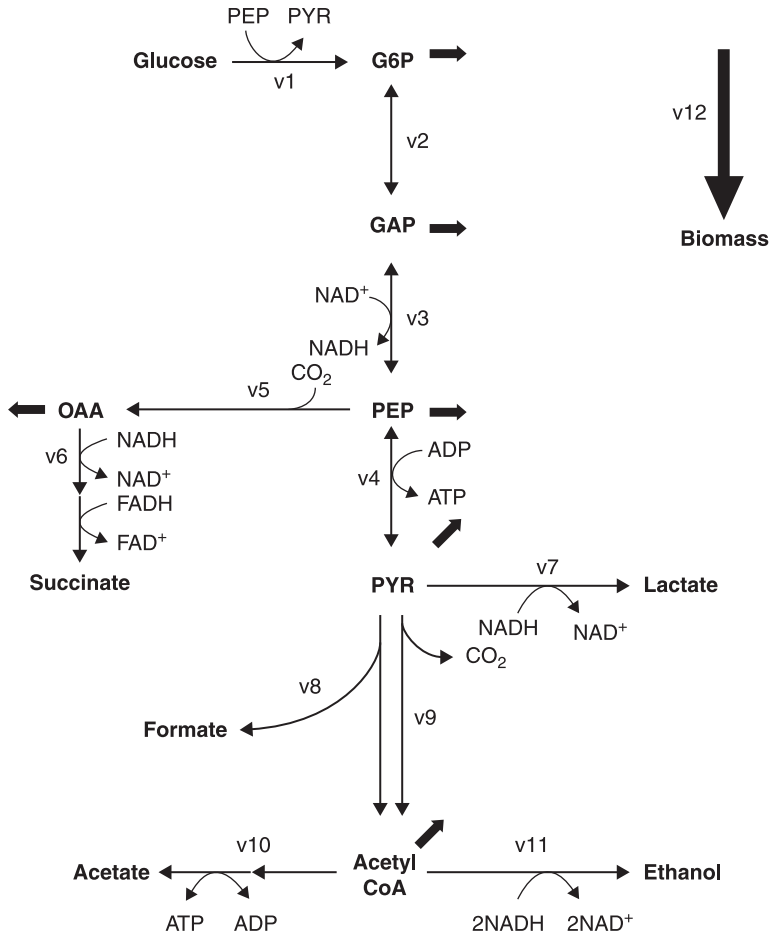

Figure 4.10 General metabolic pathway of *E. coli* under oxygen-limited conditions. The fluxes through each pathway are designated v_1–v_{12}

glycolysis. Correspondingly, the GAPDH expression level is also significantly high in these two strains. These results indicate that the demand for glycolytic flux dominates over the intracellular redox balance. The high glycolytic flux results in a high intracellular NADH/NAD$^+$ ratio, and subsequently lactate is produced to regenerate NAD$^+$ so that the glycolysis continues to work (Zhu and Shimizu, 2005).

The lactate producing flux (v_7) in the *ppc* mutant is lower than those of the other two lactate producing mutants, such as *pflA* and *pta* mutants.

Published by Woodhead Publishing Limited, 2013

Table 4.11 Effect of a single-gene knockout on the flux distribution

	Fluxes (mmol/g DCW/h)											
	v_1	v_2	v_3	v_4	v_5	v_6	v_7	v_8	v_9	v_{10}	v_{11}	v_{12}
Wild	6.30±0.06	5.90±0.07	11.73±0.10	3.85±0.09	1.39±0.09	0.42±0.06	0.09±0.06	7.28±0.35	1.97±0.23	4.47±0.12	3.52±0.11	3.94±0.10
Δ*pflA*	8.15±0.06	7.58±0.07	14.93±0.10	5.71±0.10	0.78±0.10	0.18±0.11	11.69±0.7	0.00±0.00	1.64±0.11	0.46±0.2	0.45±0.10	1.62±0.11
Δ*pta*	6.51±0.06	5.79±0.06	11.27±0.10	3.03±0.10	1.37±0.10	0.77±0.10	7.36±0.83	0.70±0.06	0.92±0.10	0.61±0.3	0.31±0.12	1.26±0.12
Δ*ppc*	1.59±0.02	1.48±0.02	2.90±0.03	1.12±0.02	0.14±0.02	0.00±0.03	1.13±0.1	0.62±0.07	0.66±0.03	0.72±0.08	0.45±0.06	0.20±0.02
Δ*adhE*	1.10±0.02	1.04±0.02	2.05±0.03	0.76±0.04	0.15±0.03	0.07±0.02	0.23±0.03	0.53±0.06	1.03±0.05	1.45±0.05	0.00±0.02	0.27±0.04
Δ*pykF*	9.02±0.07	7.05±0.07	13.21±0.07	0.00±0.00	3.21±0.33	1.54±0.23	0.13±0.2	7.82±0.29	2.56±0.43	7.75±0.4	2.93±0.31	2.48±0.23

It is consistent with the lower glycolytic flux in the *ppc* mutant. As compared to the parent strain, the lactate production rate in the *ppc* mutant is about 7 times higher. However, the lactate yield is about 30-fold higher as compared to that of the parent strain (Table 4.8). Comparing the glucose uptake rates (v_1) in these two strains, the glycolytic flux in the *ppc* mutant is about 17% of that in the wild type. Table 4.12 shows that the percentage of the flux partitioned at the pyruvate node to lactate is significantly higher in the *ppc* mutant, as compared to the parent strain. The ratio is even higher than the other lactate producing strains, such as *pflA* and *pta* mutants. It is known that the reactions through LDH and Pfl are competing with each other (Böck and Sawers, 1996). The high intracellular NADH/NAD^+ ratio is a plausible reason for the significantly up-regulated LDH activity and down-regulated Pfl activity in the *pflA* and *pta* mutants.

The flux through Ppc (v_5) in the *pykF* mutant is about 2.6-fold that in the parent strain. From enzyme activity data, Ppc activity in the *pykF* mutant is up-regulated by about 60% as compared to the parent strain. The reason for the high Ppc flux may be due to high PEP concentration and synergistic activation by FDP (Table 4.10) (Smith et al., 1980; McAlister et al., 1981). The Ppc flux is low in *ppc* and *adhE* mutants, as compared to the parent strain, which is consistent with the higher relative flux going toward pyruvate at the PEP node (Table 4.12).

Table 4.12 Effect of a single-gene knockout on flux partitions

	Percentage partitioned at PEP node to pyruvate $\left(\frac{v_1+v_4}{v_1+v_4+v_4}\right)\times 100$	Percentage partitioned at pyruvate node to lactate $\left(\frac{v_7}{v_7+v_8+v_9}\right)\times 100$	Percentage partitioned at AcCoA node to acetate $\left(\frac{v_{10}}{v_{10}+v_{11}}\right)\times 100$
Wild type	88.0	1.0	55.9
Δ*pflA*	94.7	87.7	50.5
Δ*pta*	87.4	82.0	66.3
Δ*ppc*	95.1	46.9	61.5
Δ*adhE*	92.5	12.8	100.0
Δ*pykF*	73.8	0.0	72.6

Published by Woodhead Publishing Limited, 2013

Since the product of the reaction through Ppc is OAA, which is the precursor of some amino acids such as aspartate and asparagine, the low Ppc flux is consistent with the low biomass synthesis flux (v_{12}) in these two mutants. As a consequence, the glycolytic flux, which is used to supply energy for cell growth, is low in *ppc* and *adhE* mutants (Zhu and Shimizu, 2005).

Table 4.12 shows that the flux partitioning at the AcCoA node is significantly different in *adhE* and *pykF* mutants, as compared to the others. The reaction through ADH to ethanol is blocked by the *adhE* knockout gene, and therefore AcCoA can only be used for cell growth and acetate production. In the *pykF* mutant, the flux distribution at the AcCoA node is determined by the expression of Ack and ADH. The Ack expression in *pflA* and *pta* mutants is significantly up-regulated. However, the ratios of the flux partitioned to acetate are 50.5% and 66.3% in *pflA* and *pta* mutants, respectively, which are little changed by high Ack activity in these two strains, as compared to the ratio of 55.9% in the parent strain (Zhu and Shimizu, 2005).

Pyruvate is competed for by the reactions through Pfl and LDH. In wild-type *E. coli*, the LDH reaction is not as competitive as the reaction through Pfl and, therefore, acetate and formate are the main metabolites instead of lactate (Kessler et al., 1992; Kessler and Knappe, 1996). However, the knockouts of *pflA, pta*, and *ppc* genes significantly change enzyme expression and intracellular states, resulting in over-production of lactate. The knockout of the *pflA* gene blocks the pyruvate assimilation through the Pta–Ack and ADH pathways, which are commonly used for ATP production and NADH re-oxidation, respectively, in the wild-type *E. coli*. Since the glycolytic flux is promoted by anaerobiosis with a higher ATP requirement, lactate is produced to satisfy both the stoichiometric and intracellular redox balances (Zhu and Shimizu, 2004). Looking at the enzyme activity results (Table 4.9), the LDH activity is up-regulated by about 3-fold, as compared to the parent strain. Similar phenomena can be seen in the *pta* mutant. The Pfl activity in the *pta* mutant is about one-fifth of that in the parent strain, and LDH activity is up-regulated by more than 2-fold. As a result, the flux through Pfl (v_8) is about one-tenth of that in the parent strain (Table 4.11), and the ratio of flux partitioned at the pyruvate node to lactate is comparable to that in the *pflA* mutant (Table 4.12).

The competition for PYR by reactions through Pfl and LDH is shown in Figure 4.11, by plotting the LDH fluxes against Pfl and LDH activity

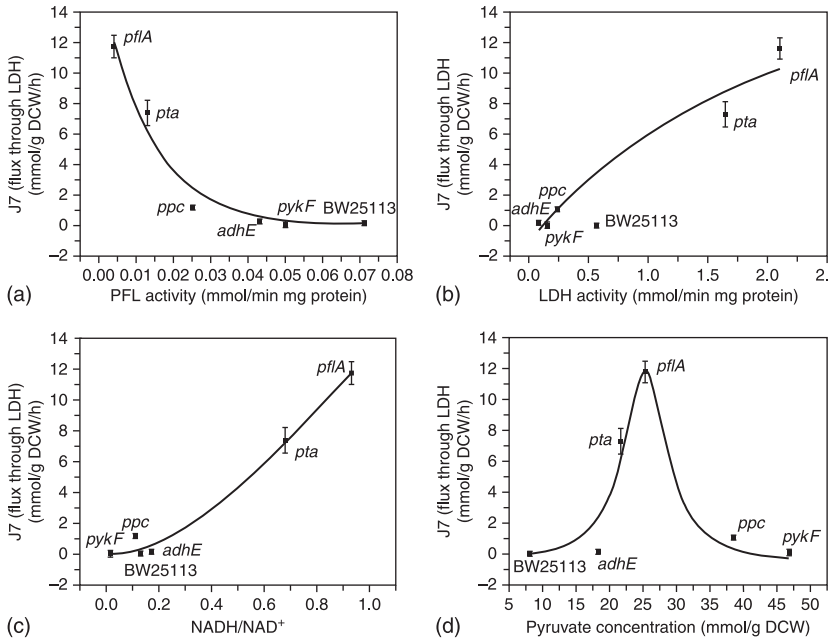

Figure 4.11 **Factors influencing lactate producing flux. The effects of Pfl, LDH activities, NADH/NAD$^+$ ratio, and intracellular pyruvate concentration on flux toward lactate generation are represented in (a), (b), (c), and (d), respectively. Error bars indicate deviation of fluxes**

in different strains. The LDH flux increases as the Pfl activity becomes low. The change in LDH activity also contributes to the LDH flux. The deviation index of the specific flux J with respect to the enzyme E, defined as $(\Delta J/\Delta E)(Er/Jr)$ (Small and Kacser, 1993), may be used to compare the effects of LDH and Pfl activity on the lactate production. The deviation index is related to the control coefficient, and can be used as a measure of the effects of large changes in enzyme activities or other effectors on the flux (Stephanopoulos et al., 1998; Yang and San, 1999). The superscript r refers to the reference value at the new perturbed state. Since the enzyme activity varies largely to the wild-type state, the deviation indexes may be evaluated using the neighboring points as the original state (Table 4.11). Table 4.13 shows that LDH controls lactate production in the *pflA* mutant, where the deviation index for LDH flux with respect to Pfl is low due to the low Pfl activity value. Pfl significantly

Published by Woodhead Publishing Limited, 2013

dominates over LDH in the cases of *ppc* and *adhE* mutants. This may explain why there is still high lactate production in *ppc* and *adhE* mutants, although LDH activity is lower, as compared to the parent strain. The large value of the deviation index of the *adhE* mutant for the LDH flux with respect to Pfl is due to the low LDH flux value in this mutant. This result is in contrast with the previous work on *Lactococcus lactis* (Andersen et al., 2001), which shows that the control by lactate dehydrogenase on lactate production is close to zero. In their study, LDH activity ranges from 1% to 133% of that in the wild type. Here, similar results may be seen when LDH activity is comparable or lower than that in the wild type. However, further amplification of LDH activity to 3–5-fold higher by corresponding gene modification shows that the amplified LDH regained control on the LDH flux. Similar results may be seen in Yang and San (1999), who show that the over-expression of LDH from 1.3 to 15.3 units significantly increases lactate production and the deviation index is about 0.57 and 1.16, respectively, according to different original states. Here, the simultaneous decrease in the activity of Pfl also contributes to the increase in LDH flux. Table 4.13 shows that LDH and Pfl activity have approximately equal control on lactate production in the *pta* mutant.

Looking at the relationship between the flux through LDH (v_7) and the intracellular NADH/NAD$^+$ ratio (Figure 4.11C), it is clear that the high flux toward lactate production or the high LDH activity might be induced by the high intracellular redox balance pressure. Similar to the deviation index, the sensitivity index, $(\Delta J/\Delta P)(Pr/Jr)$, may be defined (Small and

Table 4.13 Deviation index for LDH flux

New state	Original state	Deviation index for LDH flux	
		$\left(\frac{\Delta J_7}{\Delta LDH}\right)\left(\frac{LDH^r}{J_7^r}\right)$	$\left(\frac{\Delta J_7}{\Delta Pfl}\right)\left(\frac{Pfl^r}{J_7^r}\right)$
Δ*pflA*	Δ*pta*	1.64	−0.16
Δ*pta*	Δ*ppc*	0.94	−0.92
Δ*ppc*	Δ*adhE*	0.80	−1.11
Δ*adhE*	Δ*ppc*	0.00	−9.35
Δ*pykF*	Wild type	−0.05	−0.73

Kacser, 1993; Yang et al., 2001), where ΔP is the perturbation of the intracellular metabolite concentration. In *pflA* and *pta* mutants, the sensitivity indexes for LDH flux with respect to NADH/NAD^+ ratio are 1.37 and 1.28, respectively, which indicate that the higher intracellular redox balance pressure causes more lactate formation. The effect of intracellular pyruvate concentration on LDH flux (v_7) is shown in Figure 4.11d. Although the flux toward lactate production increases as the pyruvate concentration increases, further increase in pyruvate concentration reduces the LDH flux in *ppc* and *pykF* mutants. The pyruvate is the substrate for LDH reaction. However, the high lactate production in *pflA* and *pta* mutants cannot be simply explained by the high intracellular pyruvate concentration. The results indicate that the high LDH activity and NADH/NAD^+ ratios contribute more than intracellular pyruvate to the high LDH flux in these two strains. It should be noted that the high pyruvate concentration in the mutants is the result of several factors such as glucose uptake rate, Pfl, and LDH activity, etc.

In the parent strain and its several mutants, such as *pflA, pta*, and *ppc* knockout strains, the percentage of the flux partitioned at the AcCoA node to acetate shows a small change, which varies (Table 4.12) (AcCoA used for biomass synthesis is not considered to calculate the flux partition at the AcCoA node). Studies of strictly anaerobic cultivation have shown that the ratio of acetate production and ethanol production is about 1:1 in the wild-type *E. coli* (Alexeeva et al., 2000; Vemuri et al., 2002). This ratio may be affected by the available AcCoA and the intracellular redox balance caused by the residual activity of PDH (Alexeeva et al., 2000; De Graef et al., 1999). The flux partition at the AcCoA node is different in *pykF* and *adhE* mutants (Table 4.11). Most AcCoA is forced by the Pta–Ack pathway to form acetate in the *adhE* mutant, since the ethanol formation pathway is blocked. Note the higher acetate production in the *pykF* mutant as compared to the parent strain. It has been shown that the higher intracellular pyruvate concentration favors acetate production (Yang et al., 2001). The feed and intracellular pyruvate levels effect the redistribution of metabolic fluxes in *E. coli* (Yang et al. 2001). However, this may not be the case in the present example. No AcCoA accumulation occurs, while it is expected in the mutants such as *pta* and *adhE* strains. The relationship between the Pta–Ack flux and the intracellular AcCoA concentration can be seen in Figure 4.12a. The sensitivity indexes for the Pta–Ack flux with respect to AcCoA concentration in the *pykF* mutant and the parent strain are 0.93 and 0.79, respectively.

Published by Woodhead Publishing Limited, 2013

This indicates that AcCoA availability is a limiting factor for relatively high flux toward acetate formation. Figure 4.12b shows that the Pta–Ack flux increases as Pfl activity increases. The control of Pfl on the Pta–Ack flux is not significant in *pflA* and *pta* mutants, which show low acetate production. The deviation indexes for the Pta–Ack flux with respect to Pfl activity are 0.15 and 0.36 for *pflA* and *pta* mutants, respectively. However, it is shown that the LDH flux is significantly controlled by LDH in these two strains. Therefore, the

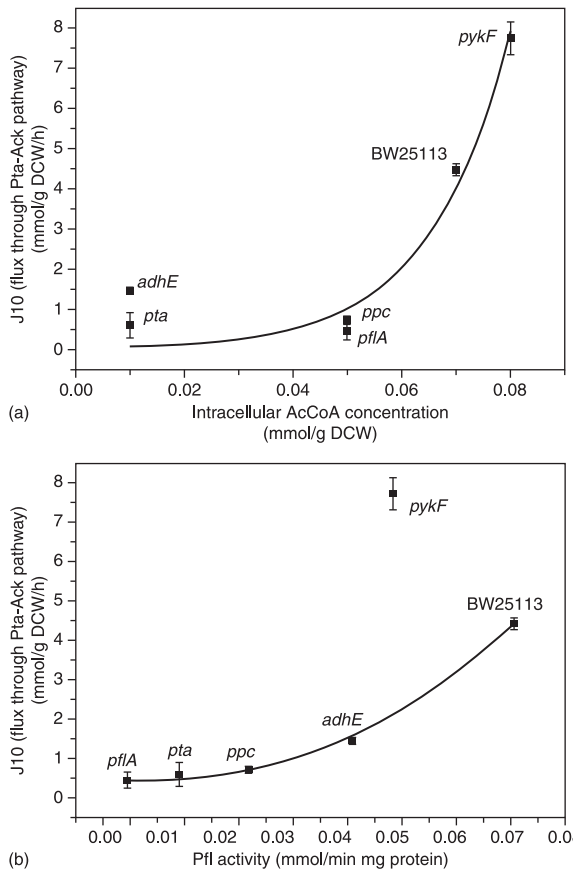

Figure 4.12 **Factors influencing flux through Pta–Ack pathway. The effects of intracellular AcCoA concentration and Pfl activity are shown in a and b, respectively. Error bars indicate deviation of fluxes**

flux through Pfl, the competitive process of LDH, is low due to high LDH activity in *pflA* and *pta* mutants. Therefore, the Pta–Ack flux depends on the flux through Pfl for AcCoA supply (Zhu and Shimizu, 2005).

The reaction from PEP to OAA through Ppc is the main pathway to replenish OAA in *E. coli* under oxygen-limited conditions (Vemuri et al., 2002). Succinate is derived from OAA, and two equivalents of NADH are required for 1 mole of succinate production. In PTS, PEP is used to transport phosphate for glucose utilization. The reaction through Pyk also uses PEP to produce PYR and ATP. It has been reported that glycolysis is down-regulated in the *pykF* mutant *E. coli* under aerobic condition (Emmerling et al., 2002; Siddiquee et al., 2004a,b). However, when the *pykF* mutant is cultivated under anaerobic condition, the specific glucose uptake rate increases by about 50%, as compared to the parent strain. Flux through glycolysis is reported to be controlled by the ATP requirement in *E. coli*. By optimizing additional ATP hydrolysis, the glycolytic flux increases significantly (Koebmann et al., 2002). Under anaerobic conditions, ATP is considered to be produced by the reactions through the Pyk and Ack pathway due to ATP balance. It can be seen that the flux through the Ack reaction is controlled by the flux through Pfl instead of Ack activity. The changes in the glycolytic flux and the flux through Pyk with respect to Pyk activity are shown in Figure 4.13. The deviation index for the Pyk flux with respect to Pyk activity is 1 for all the strains, which indicates that this flux is controlled by the Pyk enzyme. The Pyk enzyme also shows significant control on the glycolytic flux (Figure 4.13b). The deviation indexes for glycolytic flux (v_3) with respect to Pyk activity vary from 0.60 to 1.16 in the strains considered, except for the *pykF* mutant, in which the glycolytic flux is obviously independent of Pyk activity (Zhu and Shimizu, 2007).

Since OAA is one of the important precursors for the cell synthesis, the flux through Ppc is considered to affect cell growth. This indicates that the single gene knockout significantly reduce the growth. This can also be shown by the low biomass yields in the mutants (Table 4.8). Ppc activity in *pflA* is high compared to other strains (Table 4.9). This may be due to intracellular redox balance pressure. Although Ppc activity is high, the intracellular PEP concentration is low in the *pflA* mutant as compared to other strains. Therefore, the flux through Ppc (v_5) is relatively low in this mutant.

Published by Woodhead Publishing Limited, 2013

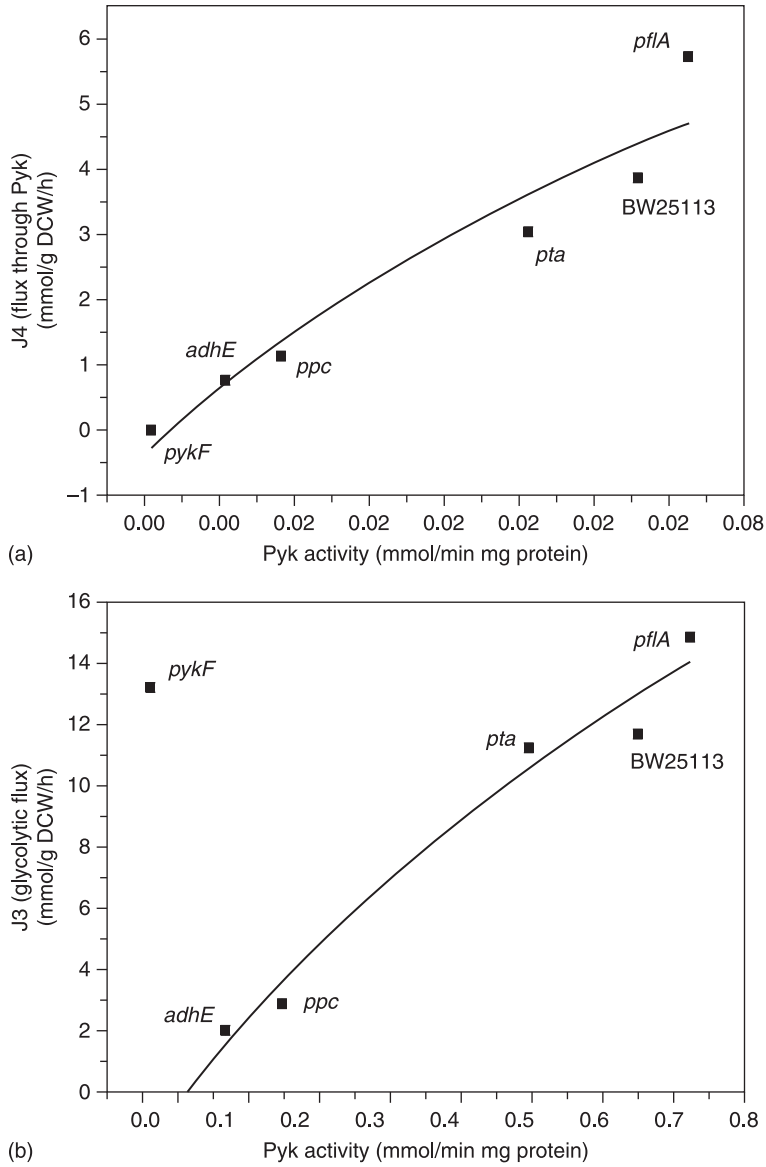

Figure 4.13 **The effect of Pyk activity on: (a) Pyk flux; and (b) glycolytic flux. Error bars indicate deviation of fluxes**

4.5 References

Akazawa, T. and Okamoto, K (1980) 'Biosynthesis of sucrose', in: *The Biochemistry of Plants*, Vol. 3, edited by J. Preiss. New York: Academic Press. pp. 199–218.

Alexeeva, S., de Kort, B., Sawers, G., Hellingwerem, K.J., and de Mattos, M.J.T. (2000) 'Effects of limited aeration and of the ArcAB system on intermediary pyruvate catabolism in *Escherichia coli*', *Journal of Bacteriology*, 182: 4934–40.

Andersen, H.W., Pedersen, M.B., Hammer, K., and Jensen, P.R. (2001) 'Lactate dehydrogenase has no control on lactate production but has a strong negative control on formate production in *Lactococcus lactis*', *European Journal of Biochemistry*, 268: 6379–89.

Aristidou, A.A., San, K.Y., and Bennett, G.N. (1999) 'Metabolic flux analysis of *Escherichia coli* expressing the *Bacillus subtilis* acetolactate synthase in batch and continuous cultures', *Biotechnology and Bioengineering*, 63: 737–49.

Avron, M. (1989) 'Photosynthetic electron transport and photophosphorylation', in: *The Biochemistry of Plants*, vol. 8, edited by M.D. Hatch and N.K. Boardman. New York: Academic Press. pp. 164–89.

Bailey, J.E. (1991) 'Toward a science of metabolic engineering', *Science*, 252: 1668–75.

Böck, A. and Sawers, G. (1996) 'Fermentation', In: Escherichia coli *and* Salmonella. *Cellular and Molecular Biology*, 2nd edition, edited by F.C. Neidhardt et al. Washington DC: American Society for Microbiology Press.

Bonarius, H.P.J., Hatzimanikatis, V., Meesters, H.P.H, de Gooijer, C.D., Schmid, G., and Tramper, J. (1996) 'Metabolic flux analysis of hybridoma cells in different culture media using mass balances', *Biotechnology and Bioengineering*, 50: 299–318.

Borowitzka, MA. (1988) 'Vitamins and fine chemicals from microalgae', in: *Microalgal Biotechnology*, edited by M.A. Borowitzka and L.J. Borowitzka. Cambridge: Cambridge University Press. pp. 153–96.

Castelfranco, P.A. and Beale, S.I. (1981) 'Chlorophyll biosynthesis', in: *The Biochemistry of Plants*, vol. 8, edited by M.D. Hatch and N.K. Boardman. New York: Academic Press. pp. 376–414.

Copeland, L. and Turner, J.F. (1987) 'The regulation of glycolysis and the pentose phosphate pathway,' in: *The Biochemistry of Plants*, vol. 11, edited by D.D. Davies. New York: Academic Press. pp. 107–25.

de Graef, M.R., Alexeeva, S., Snoep, J.L., and de Mattos, M.J.T. (1999) 'Steady-state internal redox state (NADH/NAD) reflects the external redox state and is correlated with catabolic adaptation in *Escherichia coli*', *Journal of Bacteriology*, 181: 2351–7.

de Gucht, L.P.E. and van der Plas, L.H.W. (1995) 'Growth kinetics of glucose-limited *Petunia hybrida* cells in chemostat cultures: Determination of experimental values for growth and maintenance parameters', *Biotechnology and Bioengineering*, 47: 42–52.

Douce, R., Brouquisse, R., and Journet, E.P. (1987) 'Electron transfer and oxidative phosphorylation in plant mitochondria', in: *The Biochemistry of Plants*, vol. 11, edited by D.D. Davies. New York: Academic Press. pp. 177–207.

Published by Woodhead Publishing Limited, 2013

Droop, M.R. (1974) 'Heterotrophy of carbon', in: *Algal Physiology and Biochemistry*, edited by W.D.P. Stewart. University of California Press. pp. 530–60.

Dry, I.B., Bryce, J.H., and Wiskich, J.T. (1987) 'Regulation of mitochondrial respiration', in: *The Biochemistry of Plants*, vol. 11, edited by D.D. Davies. New York: Academic Press. pp. 214–7.

Edwards, J.S. and Palsson, B.O. (2000) 'The *Escherichia coli* MG1655 *in silico* metabolic genotype: Its definition, characteristics, and capabilities', *Proceedings of the National Academy of Sciences of USA*, 97: 5528–33.

Edwards, J.S., Ibarra, R.U., and Palsson, B.O. (2001) '*In silico* predictions of *Escherichia coli* metabolic capabilities are consistent with experimental data', *Nature Biotechnology*, 19: 125–30.

Emmerling, M., Dauner, M., Ponti, A., Fiaux, J., Hochuli, M. et al. (2002) 'Metabolic flux responses to pyruvate kinase knockout in *Eshcherichia coli*', *Journal of Bacteriology*, 184: 152–64.

Fowden, L. (1962) 'Amino acids and proteins', in: *Physiology and Biochemistry of Algae*, edited by R.A. Lewin. New York: Academic Press. pp. 189–206.

Garrigues, C., Loubiere, P., Lindle, N.D., and Cocaign-bousquet, M. (1997) 'Control of the shift from homolactic acid to mixed-acid fermentation in *lactococcus lactis*: predominant role of the NADH/NAD+ ratio', *Journal of Bacteriology*, 179: 5282–7.

Glombitza, K.W. and Koch, M. (1989) 'Secondary metabolites of pharmaceutical potential', in: *Algal and Cyanobacterial Biotechnology*, edited by R.C. Cresswell, T.A.V. Rees, and H. Shah. New York: Longman. pp. 161–219.

Graham, D. (1980) 'Effects of light on dark respiration', in: *The Biochemistry of Plants*, vol. 2, edited by D.D. Davies. New York: Academic Press. pp. 526–75.

Greenbaum, E., Lee, J.W., Tevault, C.V., Blankinshi, S.L., and Mets, L.J. (1995) 'CO_2 fixation and photoevolution of H_2 and O_2 in a mutant of Chlamydomonas lacking photosystem I', *Nature*, 376: 438–41.

Grima, E.M., Camacho, F.G., Perez, J.A.S, Fernandez, F.G.A., and Sevilla, J.F. (1997) 'Evaluation of photosynthetic efficiency in microalgal cultures using averaged irradiance', *Enzyme and Microbial Technology*, 21: 375–81.

Heldt, H.W. and Flugge, U.I. (1987) 'Subcellular transport of metabolites in plant cells', in: *The Biochemistry of Plants*, vol. 12, edited by D.D. Davies. New York: Academic Press. pp. 50–80.

Hu, Q., Kurano, N., Kawachi, M., Iwasaki, I., and Miyachi, S. (1998) 'Ultrahigh-cell-density culture of a marine green alga *Chlorococcum littorale* in a flat-plate photobioreactor', *Applied Microbiology and Biotechnology*, 49: 652–5.

Ibarra, R.U., Edwards, J.S., and Palsson, B.O. (2002) '*Escherichia coli* K-12 undergoes adaptive evolution to achieve in silico predicted optimal growth', *Nature*, 420: 186–9.

Kelly, G.J. and Latzko, E. (1980) 'The cytosol', in: *The Biochemistry of Plants*, vol. 1, edited by N.E. Tolbert. New York: Academic Press. pp. 183–205.

Kessler, D. and Knappe, J. (1996) 'Anaerobic dissimilation of pyruvate', In: Escherichia coli *and* Salmonella. *Cellular and Molecular Biology*, 2nd edition,

edited by F.C. Neidhardt et al., Washington DC: American Society of Microbiology Press.
Kessler, D., Herth, W., and Knappe, J. (1992) 'Ultrastructure and pyruvate formate-lyase radical quenching property of the multi-enzymatic adhE protein of *Escherichia coli*', *Journal of Biological Chemistry*, 267: pp. 18073–9.
Koebmann, B.J., Westerhoff, H.V., Snoep, J.L., Nilsson, D., and Jensen, P.R. (2002) 'The glycolytic flux in *Escherichia coli* is controlled by the demand for ATP', *Journal of Bacteriology*, 184: 3909–16.
Kurano, N, and Miyachi, S. (1995) 'Fixation and utilization of carbon dioxide by microalgal photosynthesis', *Biotechnology and Bioengineering*, 36: 689–92.
Lee, H.Y. and Erickson, L.E. (1987) 'Theoretical and experimental yields for photo-autotrophic mixotrophic and photo-heterotrophic growth', *Biotechnology and Bioengineering*, 29: 476–81.
Lee, C.G. and Palsson, B.O. (1994) 'High-density algal photo-bioreactors using light-emitting diodes', *Biotechnology and Bioengineering*, 44: 1161–7.
Lloyd, D. (1974) 'Dark respiration', in: *Algal Physiology and Biochemistry*, edited by W.D.P. Stewart. University of California Press. pp. 505–30.
Mandalam, R.K. and Palsson, B.O. (1998) 'Elemental balancing of biomass and medium composition enhances growth capacity in high-density *Chlorella vulgaris* cultures', *Biotechnology and Bioengineering*, 59: pp. 605–11.
McAlister, L.E., Evans, E.L., and Smith, T.E. (1981) 'Properties of a mutant *Escherichia coli* phosphoenolpyruvate carboxylase deficient in co-regulation by intermediary metabolites', *Journal of Bacteriology*, 146: 200–8.
Miflin, B.J. and Lea, P.J. (1980) 'Ammonia assimilation', in: *The Biochemistry of Plants*, vol. 5, edited by B.J. Miflin. New York: Academic Press. pp. 169–99.
Morris, I. (1974) 'Nitrogen assimilation and protein synthesis', in: *Algal Physiology and Biochemistry*, edited by W.D.P. Stewart. University of California Press. pp. 583–610.
Nichols, B.W. (1965) 'Light induced changes in the lipids of *Chlorella vulgaris*', *Biochemistry and Biophysics ACTA*, 106: 274–9.
Nishimura, T., Pachpande, R.R., and T. Iwamura, T. (1988) 'A heterotrophic synchronous culture of *Chlorella*', *Cell Structure Function*, 13: 207–15.
Ogawa, T, and Aiba, S. (1981) 'Bioenergetic analysis of mixotrophic growth in *Chlorella vulgaris* and *Scenedesmus acutus*', *Biotechnology and Bioengineering*, 23: 1121–32.
Ogbonna, J.C. and Tanaka, H. (1996) 'Night biomass loss and changes in biochemical composition of cells during light/dark cyclic culture of *Chlorella pyrenoidosa*', *Journal of Fermentation and Bioengineering*, 82: 558–64.
Palsson, B. (2009) 'Metabolic systems biology', FEBS Letters, 583: 3900–3904.
Price, N.D., Papin, J.A., Schilling, C.H., and Palsson, B,O. (2003) 'Genome-scale microbial in silico models: the constraints-based approach', *Trends in Biotechnology*, 21: 162–9.
Raymond, P., Gidrol, X., Salon, C., and Pradet, A. (1987) 'Control involving adenine and pyridine nucleotides', in: *The Biochemistry of Plants*, vol. 11, edited by D.D. Davies. New York: Academic Press. pp. 130–68.
Rees, T.A. (1980) 'Assessment of the contribution of metabolic pathways to plant respiration', in: *The Biochemistry of Plants*, vol. 2, edited by D.D. Davies. New York: Academic Press. pp. 1–27.

Published by Woodhead Publishing Limited, 2013

Rees, T.A. (1987) 'Compartmentation of plant metabolism', in: *The Biochemistry of Plants*, vol. 12, edited by D.D. Davies. New York: Academic Press. pp. 87–113.

Schilling, C.H. and Palsson, B.O. (1998) 'The underlying pathway structure of biochemical reaction networks', *Proceedings of the National Academy of Sciences of USA*, 95: 4193–8.

Schuetz, R., Kuepfer, L., and Sauer, U. (2007) 'Systematic evaluation of objective functions for predicting intracellular fluxes in *Escherichia coli*', *Molcular Systems Biology*, 3: 1–14.

Siddiquee, K.A.Z., Arauzo-Bravo, M., and Shimizu, K. (2004a) 'Metabolic Flux Analysis of *pykF* gene knockout *Escherichia coli* based on ^{13}C-labeled experiment together with measurements of enzyme activities and intracellular metabolite concentrations', *Applied Microbiology and Biotechnology*, 63: 407–17.

Siddiquee, K.A.Z., Arauzo-Bravo, M., and Shimizu, K. (2004b) 'Effect of pyruvate kinase (*pykF* gene) knockout mutation on the control of gene expression and metabolic fluxes in *Escherichia coli*', *FEMS Microbiology Letters*, 235: 25–33.

Small, J.R. and Kacser, H. (1993) 'Response of metabolic systems to large changes in enzyme activities and effectors: 1. The linear treatment of unbranched chains', *European Journal of Biochemistry*, 213: 613–24.

Smith, T.E., Balasubramanian, K.A., and Beezley, A. (1980) '*Escherichia coli* phoshpoenol -pyruvate carboxylase: Studies on the mechanism of synergistic activation by nucleotides', *Journal of Biological Chemistry*, 255: 1635–42.

Stephanopoulos, G.N. (1999) 'Metabolic fluxes and metabolic engineering', *Metabolic Engineering*, 1: 1–11.

Stephanopoulos, G.. and Vallino, J.J. (1991) 'Network rigidity and metabolic engineering in metabolite overproduction', *Science*, 252: 1675–81.

Stephanopoulos, G.N., Aristidou, A.A., and Nielsen, J. (1988) 'Metabolic control analysis', in: *Metabolic Engineering. Principles and Methodologies*, edited by G.N. Stephanopoulos, A.A. Aristidou, and J. Nielsen. New York: Academic Press. pp. 461–533.

Storey, B.T. (1980) 'Electron transport and energy coupling in plant mitochondria', in: *The Biochemistry of Plants*, vol. 2, edited by D.D. Davies. New York: Academic Press. pp. 125–87.

Tolbert, N.E. (1980) 'Photorespiration' *The Biochemistry of Plants*, vol. 2, edited by D.D. Davies. New York: Academic Press. pp. 488–521.

Tredici, M.R. and Zittelli, G.C. (1998) 'Efficiency of sunlight utilization: Tubular versus flat photo-bioreactors', *Biotechnology and Bioengineering*, 57: 187–97.

Tsai, S.P. and Lee, Y.H. (1988) 'Application of metabolic pathway stoichiometry to statistical analysis of bioreactor measurement data', *Biotechnology and Bioengineering*, 32: 713–16.

Turner, J.F. and Turner, D.H. (1980) 'The regulation of glycolysis and the pentose phosphate pathway', in: *The Biochemistry of Plants*, vol. 2, edited by D.D. Davies, New York: Academic Press. pp. 279–312.

Vallino, J.J. and Stephanopoulos, G.N. (1993) 'Metabolic flux distributions in *Corynebacterium glutamicum* during growth and lysine over-production', *Biotechnology and Bioengineering*, 41: 633–46.

Vemuri, G.N., Eiteman, M.A., and Altman, E. (2002) 'Effects of growth mode and pyruvate carboxylase on succinic acid production by metabolically engineered strains of *Escherichia coli*', *Applied Environmental Microbiology*, 68: 1715–27.

Wang, N.S. and Stephanopoulos, G..N. (1983) 'Application of macroscopic balances to the identification of gross measurement errors', *Biotechnology and Bioengineering*, 25: 2177–208.

Wanka, F., Joosten, H.F.P., and de Grip, W.J. (1970) 'Composition and synthesis of DNA in synchronously growing cells of *Chlorella pyrenoidosa*', *Archives of Microbiology*, 75: 25–36.

Wiskich, T. (1980) 'Control of the Kerbs cycle', in: *The Biochemistry of Plants*, vol. 2, edited by D.D. Davies. New York: Academic Press. pp. 244–75.

Wood, B.J.B. (1974) 'Fatty acids and saponifiable lipids', in: *Algal Physiology and Biochemistry*, edited by W.D.P. Stewart. University of California Press. pp. 236–66.

Xie, L. and Wang, D.I.C. (1996) 'Energy metabolism and ATP balances in animal cell cultivation using a stoichiometrically based reaction network', *Biotechnology and Bioengineering*, 52: 591–601.

Yanagi, M., Watanabe. Y., and Saiki, H. (1995) 'CO_2 fixation by *Chlorella* sp. HA-1 and its utilization', *Biotechnology and Bioengineering*, 36: 713–16.

Yang, Y. and San, K.Y. (1999) 'Redistribution of metabolic fluxes in *Escherichia coli* with fermentative lactate dehydrogenase over-expression and deletion', *Metabolic Engineering*, 1: 141–52.

Yang, C., Hua, Q., and Shimizu, K. (2000) 'Energetics and carbon metabolism during growth of microalgal cells under photoautotrophic, mixotrophic, and cyclic light-autotrophic/dark-heterotrophic conditions', *Biochemical Engineering Journal*, 6: 87–102.

Yang, Y.T., Bennett, G.N., and San, K.Y. (2001) 'The effects of feed and intracellular pyruvate levels on the redistribution of metabolic fluxes in *Escherichia coli*', *Metabolic Engineering*, 3: 115–23.

Yuan, J., Fowler, W.U., Kimball, E., Lu, W., and Rabinowitz, J.D. (2006) 'Kinetic flux profiling of nitrogen assimilation in *Escherichia coli*', *Nature Chemical Biology*, 2: 529–30.

Zhu, J. and Shimizu, K. (2004) 'The effect of *pfl* genes knockout on the metabolism for optically pure D-lactate production by *Escherichia coli*', *Applied Microbiology and Biotechnology*, 64: 367–75.

Zhu, J. and Shimizu, K. (2005) 'Effect of a single-gene knockout on the metabolic regulation in *E. coli* for D-lactate production under microaerobic conditions', *Metabolic Engineering*, 7: 104–15.

Published by Woodhead Publishing Limited, 2013